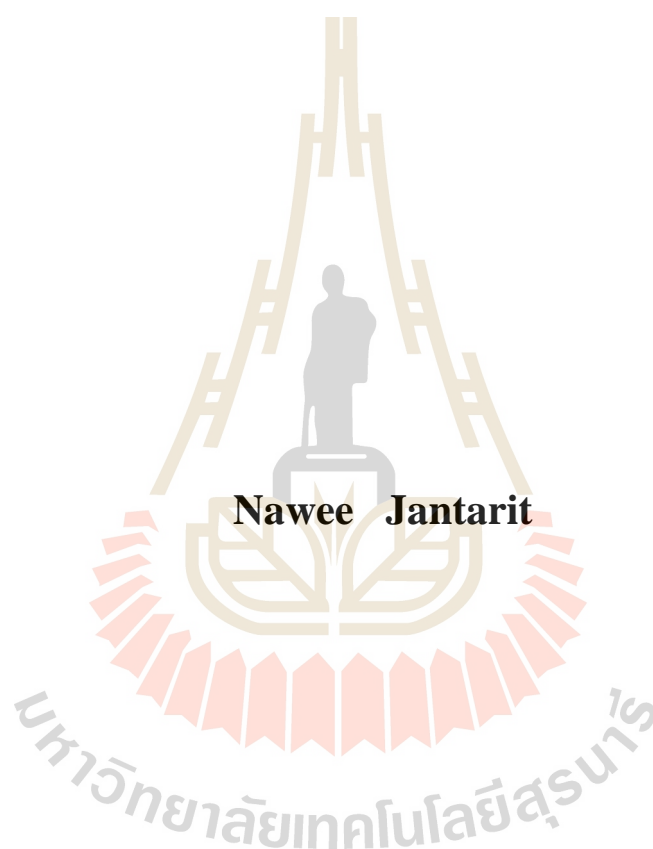


**SYNTHESIS OF EMT/FAU INTERGROWTH AND
NANOSIZED SOD ZEOLITE FROM GEL OF ZEOLITE
SODIUM X IN ETHANOL-WATER SYSTEMS**



**A Thesis Submitted in Partial Fulfillment of Requirements for the
Degree of Master of Science in Chemistry
Suranaree University of Technology
Academic Year 2019**

การสังเคราะห์ซีโอไลต์ประสานของอีเอ็มทีและเอฟเอยูและซีโอไลต์เอสโอดี
ขนาดนาโน จากเจลของซีโอไลต์โซเดียมเอ็กซ์ในระบบเอทานอลและน้ำ



นายนาวิ จันทฤทธิ

วิทยานิพนธ์นี้เป็นส่วนหนึ่งของการศึกษาตามหลักสูตรปริญญาวิทยาศาสตรมหาบัณฑิต

สาขาวิชาเคมี

มหาวิทยาลัยเทคโนโลยีสุรนารี

ปีการศึกษา 2562

**SYNTHESIS OF EMT/FAU INTERGROWTH AND NANOSIZED
SOD ZEOLITE FROM GEL OF ZEOLITE SODIUM X IN
ETHANOL-WATER SYSTEMS**

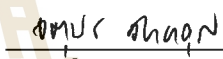
Suranaree University of Technology has approved this thesis submitted in partial fulfillment of the requirements for a Master's Degree.

Thesis Examining Committee



(Prof. Dr. James R. Ketudat-Cairns)

Chairperson




(Prof. Dr. Jatuporn Wittayakun)

Member (Thesis Advisor)



(Assoc. Prof. Dr. Sanchai Prayoonpokarach)

Member



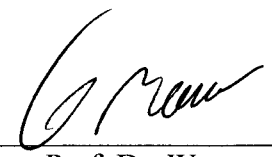
(Asst. Prof. Dr. Theeranun Siritanon)

Member



(Assoc. Prof. Ft. Lt. Dr. Kontorn Chamniprasart)

Vice Rector for Academic Affairs
and Internationalization



(Assoc. Prof. Dr. Worawat Meevasana)

Dean of Institute of Science

นาวิ จันทฤทธิ์ : การสังเคราะห์ซีโอไลต์ประสานของอีเอ็มทีและเอฟเอยูและซีโอไลต์เอสโอดีขนาดนาโนจากเจลของซีโอไลต์โซเดียมเอ็กซ์ในระบบเอทานอลและน้ำ

(SYNTHESIS OF EMT/FAU INTERGROWTH AND NANOSIZED SOD ZEOLITE FROM GEL OF ZEOLITE SODIUM X IN ETHANOL-WATER SYSTEMS).

อาจารย์ที่ปรึกษา : ศาสตราจารย์ ดร.จตุพร วิทยาคุณ, 57 หน้า.

ซีโอไลต์ประสานของอีเอ็มทีและเอฟเอยูและซีโอไลต์เอสโอดีขนาดนาโน มีประสิทธิภาพในการใช้เป็นตัวเร่งปฏิกิริยาหรือตัวรองรับ อย่างไรก็ตามวิธีการสังเคราะห์ซีโอไลต์เหล่านี้มีข้อเสียคือต้องการสารแม่แบบ ใช้อุณหภูมิสูงและใช้เวลานานในการตกผลึก ในงานนี้เป็นการรายงานการสังเคราะห์ซีโอไลต์ประสานของอีเอ็มทีและเอฟเอยูและซีโอไลต์เอสโอดีขนาดนาโนจากเจลของซีโอไลต์เอ็กซ์ในระบบเอทานอลและน้ำ ซึ่งปราศจากสารแม่แบบ ใช้อุณหภูมิต่ำกว่าและใช้เวลาสั้นลงในการตกผลึก เมื่อเทียบกับการสังเคราะห์แบบปกติของซีโอไลต์เหล่านั้น โดยตกผลึกซีโอไลต์จากเจลของซีโอไลต์เอ็กซ์ที่มีปริมาณเอทานอลและน้ำต่างกันและวิเคราะห์ของแข็งที่ได้ด้วยหลายเทคนิค เพื่อวิเคราะห์เฟส สัณฐาน ปัจจัยทางพื้นผิวและสมบัติอื่น ๆ เมื่อสังเคราะห์ซีโอไลต์ด้วยอัตราส่วนโมลของเอทานอลต่อน้ำเท่ากับ 0.045 ได้ซีโอไลต์ประสานของอีเอ็มทีและเอฟเอยูที่มีโครงสร้างกลวงและรูปร่างไม่แน่นอน ในขณะที่ซีโอไลต์ที่สังเคราะห์ด้วยอัตราส่วนโมลของเอทานอลต่อน้ำเท่ากับ 0.412 และ 0.628 ได้ซีโอไลต์เอสโอดีขนาดนาโน ยังพบอีกว่าการสังเคราะห์ที่ใช้อัตราส่วนเอทานอลต่อน้ำในช่วงกลางๆ จะได้ซีโอไลต์ที่มีเฟสผสม ซีโอไลต์ทั้งหมดมีรูพรุนแบบไมโครพอร์สที่แท้จริงและรูพรุนแบบมีโซพอร์สที่อยู่ระหว่างอนุภาคที่เกาะกัน อัตราส่วนของซิลิกอนและอะลูมิเนียมมีแนวโน้มที่จะลดลงตามการเพิ่มขึ้นของอัตราส่วนโมลของเอทานอลและน้ำ กลไกที่เป็นไปได้ของการสร้างซีโอไลต์ในระบบนี้ยังถูกเสนอ วิธีการสังเคราะห์ที่รวดเร็วและเป็นมิตรต่อสิ่งแวดล้อมจะช่วยลดค่าใช้จ่าย พลังงานและของเสียอันตราย นอกจากนี้ความเข้าใจที่ดีขึ้นเกี่ยวกับผลของเอทานอลต่อการสังเคราะห์ซีโอไลต์ อาจจะเป็นแนวทางสำหรับการควบคุมเฟสและสัณฐานของซีโอไลต์อื่น ๆ

สาขาวิชาเคมี
ปีการศึกษา 2562

ลายมือชื่อนักศึกษา นาวิ จันทฤทธิ์
ลายมือชื่ออาจารย์ที่ปรึกษา จตุพร วิทยาคุณ

NAWEE JANTARIT : SYNTHESIS OF EMT/FAU INTERGROWTH AND
NANOSIZED SOD ZEOLITE FROM GEL OF ZEOLITE SODIUM X IN
ETHANOL-WATER SYSTEMS. THESIS ADVISOR : PROF. JATUPORN
WITTAYAKUN, Ph.D. 57 PP.

ZEOLITE SODIUM X/ INTERGROWTH EMT/FAU/ NANOSIZED SOD ZEOLITE/
MESOPOROUS ZEOLITE/ ETHANOL

EMT/FAU intergrowth and nanosized SOD zeolites can be used as catalysts or catalyst supports. However, their current synthesis methods have many drawbacks, including template requirement, high crystallization temperature and long crystallization time. This thesis reports the formation of EMT/FAU intergrowth and nanosized SOD zeolite synthesized from zeolite NaX gel in an ethanol-water systems. Compared with their general synthesis methods, this method can achieve without template addition with lower crystallization temperature, and shorter crystallization time. The gels of NaX zeolite with different amounts of ethanol and water were crystallized. The solid products were characterized by several techniques to analyze phase, morphology, textural parameter, and properties. The EMT/FAU intergrowth with hollow structure and undefined shapes was produced at the ethanol/water molar ratio of 0.045. The aggregation of nanocrystalline SOD zeolite was obtained at the ethanol/water molar ratios of 0.412 and 0.628. Moreover, a mixture of those phases was observed at the ethanol/water molar ratios of 0.101, 0.174, and 0.273. All samples contain both intrinsic micropores and interparticle mesopores. The Si/Al ratio tends to decrease with the ethanol/water molar ratio. The possible mechanism of the zeolite

formation in this system is proposed. The fast and environmentally friendly method will help to reduce cost, energy and hazardous waste. Additionally, the better understanding about effect of ethanol on zeolite synthesis may provide an alternative route to control phase and morphology of other zeolites.



School of Chemistry

Academic Year 2019

Student's Signature

นาง วิษณุภรณ์

Advisor's Signature

ดร.พร อุดม

ACKNOWLEDGEMENTS

First of all, I would like to express my gratitude to Prof. Dr. Jatuporn Wittayakun, my advisor, for his patience, support and help throughout all three years. He gave me motivation, guidance and enthusiasm which are special and meaningful for my research and life journey. I learned so much about research and science from his perception and will use in the near future. Without him, this project would not have happened.

I would like to acknowledge my scholarship, Development and Promotion of Science and Technology Talents Project (DPST), from the Thai government for giving me a good opportunity to conduct interesting research. I wish to thank all lecturers of the School of Chemistry for their good attitudes and suggestions. I also thank Suranaree University of Technology (SUT) for providing scientific workplace and support. Thank all members of catalysis group at SUT and friends for their friendship and help.

Last, my grateful thanks are extended to my parents, Mr. Boonmee and Mrs. Buathong Jantarit, and other family members for their unconditional love, encouragement, and support in all situations in my life.

Nawee Jantarit

CONTENTS

	Page
ABSTRACT IN THAI.....	I
ABSTRACT IN ENGLISH	II
ACKNOWLEDGEMENTS	IV
CONTENTS.....	V
LIST OF TABLES	VIII
LIST OF FIGURES	IX
CHAPTER	
I INTRODUCTION.....	1
1.1 Introduction.....	1
1.2 References.....	5
II LITERATURE REVIEW	10
2.1 Background of zeolite	10
2.1.1 Zeolite Structure	10
2.1.2 Zeolite X (FAU-type).....	12
2.1.3 Intergrowth of EMT/FAU zeolite.....	13

CONTENTS (Continued)

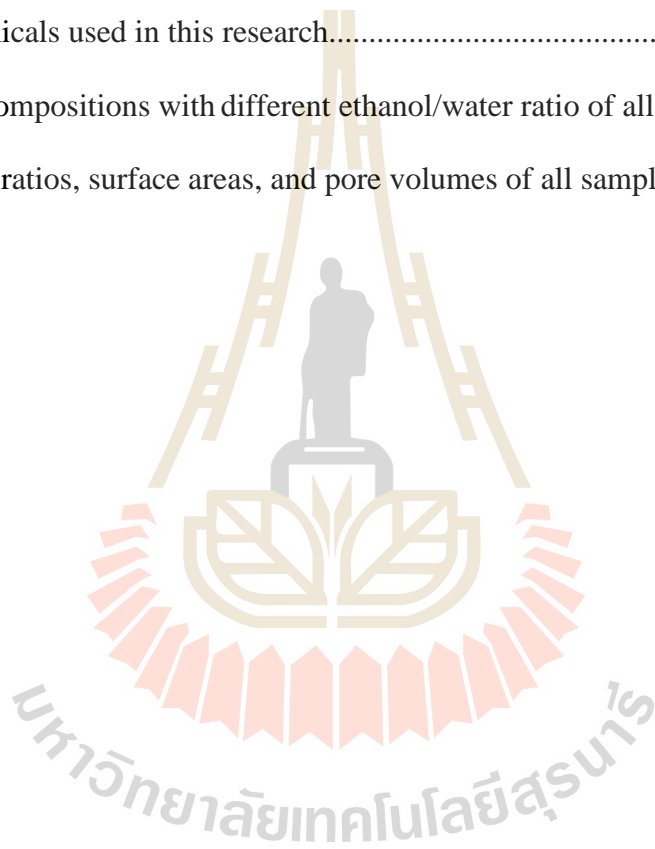
		Page
	2.1.4 Nanosized SOD zeolite	15
	2.2 Effect of ethanol on zeolite synthesis	18
	2.3 Strategy to develop the synthesis methods of EMT/FAU intergrowth and nanosized SOD zeolite	21
	2.4 References.....	23
III	EXPERIMENTAL.....	28
	3.1 Chemicals.....	28
	3.2 Zeolite synthesis in ethanol-water system	29
	3.3 Material characterization	30
	3.4 References.....	32
IV	RESULTS AND DISCUSSION	33
	4.1 Phases of samples from XRD	33
	4.2 Vibrational spectra of samples.....	36
	4.2.1 Vibrational spectra of zeolite structures.....	36
	4.2.2 Water adsorption capacity of zeolite samples	37
	4.3 Morphology of the obtained zeolites	38

CONTENTS (Continued)

	Page
4.4 Isotherms, pore size distributions, textural parameters, and Si/Al ratios of the synthesis materials.....	44
4.4 Thermal stability and water adsorption capacity of the samples.....	50
4.5 References.....	52
V CONCLUSIONS.....	56
CURRICULUM VITAE.....	57

LIST OF TABLES

Table	Page
2.1	Synthesis of nanosized SOD zeolite in basic solution..... 18
3.1	Chemicals used in this research..... 28
3.2	Gel compositions with different ethanol/water ratio of all samples..... 30
4.1	Si/Al ratios, surface areas, and pore volumes of all samples..... 47



LIST OF FIGURES

Figure	Page
2.1 Structures of Primary Building Units (PBUs) of zeolite	11
2.2 Zeolite formation by Secondary Building Units (SBUs) and Composite Building Units (CBUs).....	11
2.3 Structures of EMT, FAU and EMT/FAU intergrowth	14
2.4 Formation of SOD structure	15
4.1 XRD patterns of the resulting zeolites.....	33
4.2 FT-IR spectra of the zeolite samples	38
4.3 SEM images showing morphologies the zeolite samples.....	41
4.4 Bright-field TEM images of the aggregated zeolite particles	43
4.5 Bright-field TEM images of the EMT-FAU intergrowth from E10 gel.....	44
4.6 N ₂ adsorption-desorption isotherms of the zeolite samples	48
4.7 Pore size distribution of E00, E10, E50, and E60 samples	49
4.8 Thermogravimetric analysis of E00, E10, E20, and E50 samples	51

CHAPTER I

INTRODUCTION

Zeolite is a microporous crystalline aluminosilicate material with unique and well-defined pore sizes and channels. The interest of this work is zeolite X, which has a Si/Al ratio in the range of 1.0-1.5 and two morphologies including octahedron (Yang et al., 2006; Liu et al., 2008; Tekin et al., 2015, 2016; Chen et al., 2018) and thread-ball-like crystals (Babajide et al., 2012; Inayat et al., 2012; Musyoka et al., 2015). Zeolite X is widely used as an absorbent and ion-exchanger, due to its exclusive properties, such as high ion-exchange capacity and large surface area up to 760 m²/g (Linares et al., 2008). However, the zeolite X contains a large amount of aluminum content in the structure, which leads to reduced thermal and hydrothermal stability compared with FAU-type zeolite Y which has lower Al content (Sadeghbeigi, 2012). The low stability implies that the gel of zeolite X could be transformed easily to other types of zeolite. There are reports that different zeolite phases are produced in the synthesis of the zeolite X, for example, LTA (Ansari et al., 2014; Maatoug et al., 2017), EMT/FAU intergrowth (Gao et al., 2015), SOD (E, 2017) and GIS (Dhainaut et al., 2013; Hums et al., 2015; Musyoka et al., 2015; Maatoug et al., 2017). Those findings imply that the other zeolites could be produced from the synthesis gel of zeolite X.

Among the mentioned competitive phases of zeolite NaX, EMT/FAU intergrowth and nanosized SOD zeolite are attractive due to their application in

catalysis. Intergrowth of FAU/EMT zeolite comprises the FAU and EMT layers in the same bulk structure, resulting in a combination of advantages from both zeolites. Catalysts using the EMT/FAU intergrowth as support exhibited excellent catalytic performance in FCC gasoline hydro-upgrading (Gao et al., 2015) and n-pentane hydroisomerization (Belandría et al., 2008) compared with pure EMT and FAU supports. SOD zeolites with high surface areas, such as mesoporous SOD and nano-sized crystals have potential to act as catalyst supports or catalysts in Knoevenagel condensation, Claisen–Schmidt condensation, acetylacetone cyclization (Shanbhag et al., 2009), epoxidation of 2-cyclohexen-1-one with hydrogen peroxide (Hiyoshi, 2012), and oxidation of carbon in diesel soot combustion (Kimura et al., 2008). Nevertheless, the synthesis methods of the EMT/FAU intergrowth take a long crystallization time, up to several days and require 18-crown-6 as an organic template (Belandría et al., 2008; Gao et al., 2015). Synthesis methods of the nanosized SOD zeolite can be done both with and without an organic template. However, there are other disadvantages such as the use of high crystallization temperature (Shanbhag et al., 2009; Hiyoshi, 2012) and/or long crystallization time (Hiyoshi, 2012). The disadvantages of the synthesis methods of both zeolites usually cause high cost and energy consumption, especially for synthesis in large scale. Moreover, the organic template has to be removed by calcination, which could cause aggregates of zeolite crystals (Chen et al., 2005).

As mentioned above, EMT/FAU intergrowth and nanosized zeolite could be synthesized from the synthesis gel of zeolite X. Such an approach has advantages, including low crystallization temperature, short crystallization time, and ability to be accomplished without any template (Mintova et al., 2016). Consequently, it is

worthwhile to find a novel synthesis method of the EMT/FAU intergrowth and nanosized SOD zeolite by modifying the synthesis method or/and gel composition of zeolite X. There are several ways to alter phase, morphology, particle size and porosity of zeolite. A common method is the addition of organic additives.

Among several additives used in zeolite synthesis, ethanol is an attractive candidate. Several researchers have successfully synthesized various zeolites from ethanol-containing gels (Uguina et al., 1995; Sano et al., 2001; Oumi et al., 2003; Yao et al., 2008; Huang et al., 2011; Sharma et al., 2014; Chen et al., 2018). The presence of ethanol directly affects the properties of synthesis gels of the zeolites, such as the increasing the density, pH and Na^+ concentrations (Huang et al., 2011). Those properties influence the crystallization process, and/or morphology of the obtained zeolites (Uguina et al., 1995; Sano et al., 2001; Oumi et al., 2003; Yao et al., 2008; Huang et al., 2011; Sharma et al., 2014; Chen et al., 2018).

Moreover, there are reports about the synthesis of nanosized SOD zeolite from the synthesis gel of zeolite A in the ethanol-containing system (Yao et al., 2008; Huang et al., 2011). Ethanol slows down the zeolite crystallization process, resulting in nanosized zeolite crystals, and accelerates phase transformation to SOD zeolite (Huang et al., 2011). A formation mechanism of the zeolite from the denser gel in this system has been proposed (Huang et al., 2011). In the synthesis of the EMT/FAU intergrowth, there are no reports about the synthesis of this zeolite in the ethanol-containing system. However, Gao et al. (2015) have synthesized EMT/FAU intergrowth by increasing sodium oxide content in the synthesized gel of FAU zeolite. The addition of ethanol in the synthesis gel of zeolite NaX can increase the concentration of sodium oxide in the

aqueous phase. Since the solubility of sodium hydroxide in ethanol is lower than that in water, it could lead to the formation of EMT/FAU intergrowth. Consequently, ethanol is a potential additive in the synthesis of the EMT/FAU intergrowth and nanosized SOD zeolite from the zeolite X gel. To my knowledge, there are no reports about the synthesis of the EMT/FAU intergrowth and nanosized SOD zeolite from the zeolite X gel containing ethanol.

This thesis reports a novel approach to synthesize EMT/FAU intergrowth and nanosized SOD zeolite from zeolite X gel in the ethanol-water system. The starting synthesis gel of the zeolite X similar to the literature (Mintova et al., 2016) is modified by tuning the mole ratio of ethanol/water to crystallize the desired zeolites. Moreover, the effect of ethanol on the phase, morphology, and porosity of the zeolites is also investigated. Finally, the possible mechanism of the zeolite formation in the ethanol-water system is proposed. A better understanding of the effect of ethanol on zeolite X synthesis might provide an alternative route to control the zeolite phase and morphology.

References

- Ansari, M., Aroujalian, A., Raisi, A., Dabir, B., and Fathizadeh, M. (2014). Preparation and characterization of nano-NaX zeolite by microwave assisted hydrothermal method. **Advanced Powder Technology**. 25: 722–727.
- Babajide, O., Musyoka, N., Petrik, L., and Ameer, F. (2012). Novel zeolite Na-X synthesized from fly ash as a heterogeneous catalyst in biodiesel production. **Catalysis Today**. 190: 54–60.
- Belandr a, L. N., Gonz alez, C. S., Aguirre, F., Sosa, E., Uzc ategui, A., Gonz alez, G., Brito, J., Gonz alez-Cort es, S. L., and Imbert, F. E. (2008). Synthesis, characterization of FAU/EMT intergrowths and its catalytic performance in n-pentane hydroisomerization reaction. **Journal of Molecular Catalysis A: Chemical**. 281: 164–172.
- Chen, X., Shen, B., Sun, H., and Zhan, G. (2018). Ion-exchange modified zeolites X for selective adsorption desulfurization from Claus tail gas: Experimental and computational investigations. **Microporous and Mesoporous Materials**. 261: 227–236.
- Chen, Z., Li, S., and Yan, Y. (2005). Synthesis of template-free zeolite nanocrystals by reverse microemulsion-microwave method. **Chemistry of Materials**. 17: 2262–2266.

- Chen, Z., Chen, C., Zhang, J., Zheng, G., Wang, Y., Dong, L., Qian, W., Bai, S., and Hong, M. (2018). Zeolite Y microspheres with perpendicular mesochannels and metal@Y heterostructures for catalytic and SERS applications. **Journal of Materials Chemistry A**. 6: 6273–6281.
- Dhainaut, J., Daou, T. J., Chappaz, A., Bats, N., Harbuzaru, B., Lapisardi, G., and Chaumeil, H. (2013). Synthesis of FAU and EMT-type zeolites using structure-directing agents specifically designed by molecular modelling. **Microporous and Mesoporous Materials**. 174: 117–125.
- E, H. (2017). Synthesis of phase-pure zeolite sodalite from clear solution extracted from coal fly ash. **Journal of Thermodynamics & Catalysis**. 8(2): 1–6.
- Gao, D., Duan, A., Zhang, X., Zhao, Z., E, H., Qin, Y., and Xu, C. (2015). Synthesis of CoMo catalysts supported on EMT/FAU intergrowth zeolites with different morphologies and their hydro-upgrading performances for FCC gasoline. **Chemical Engineering Journal**. 270: 176–186.
- Hiyoshi, N. (2012). Nanocrystalline sodalite: Preparation and application to epoxidation of 2-cyclohexen-1-one with hydrogen peroxide. **Applied Catalysis A: General**. 419–420: 164–169.
- Huang, Y., Yao, J., Zhang, X., Kong, C., Chen, H., Liu, D., Tsapatsis, M., Hill, M. R., Hill, A. J., and Wang, H. (2011). Role of ethanol in sodalite crystallization in an ethanol-Na₂O-Al₂O₃-SiO₂-H₂O system. **CrystEngComm**. 13: 4714–4722.

- Hums, E., Musyoka, N. M., Baser, H., Inayat, A., and Schwieger, W. (2015). In-situ ultrasound study of the kinetics of formation of zeolites Na-A and Na-X from coal fly ash. **Research on Chemical Intermediates**. 41: 4311–4326.
- Inayat, A., Knoke, I., Spiecker, E., and Schwieger, W. (2012). Assemblies of mesoporous FAU-type zeolite nanosheets. **Angewandte Chemie - International Edition**. 51: 1962–1965.
- Kimura, R., Wakabayashi, J., Elangovan, S. P., Ogura, M., and Okubo, T. (2008). Nepheline from K_2CO_3 /nanosized sodalite as a prospective candidate for diesel soot combustion. **Journal of the American Chemical Society**. 130: 12844–12845.
- Linares, C. F., Valenzuela, E., Ocanto, F., Pérez, V., Valbuena, O., and Goldwasser, M. R. (2008). K^+ and Ca^{2+} modified Na-X zeolites as possible bile acids sequestrant. **Journal of Materials Science: Materials in Medicine**. 19: 2023–2028.
- Liu, S., Cao, X., Li, L., Li, C., Ji, Y., and Xiao, F. (2008). Preformed zeolite precursor route for synthesis of mesoporous X zeolite. **Colloids and Surfaces A: Physicochemical and Engineering Aspects**. 318: 269–274.
- Maatoug, N., Delahay, G., and Tounsi, H. (2017). Valorization of vitreous China waste to EMT / FAU , FAU and Na-P zeotype materials. **Waste Management**. 74: 267–278.
- Mintova, S., and Barrier, N. (2016). Verified syntheses of zeolitic materials. **Commission of the International Zeolite Association**.

- Musyoka, N. M., Petrik, L. F., Hums, E., Kuhnt, A., and Schwieger, W. (2015). Thermal stability studies of zeolites A and X synthesized from South African coal fly ash. **Research on Chemical Intermediates**. 41: 575–582.
- Oumi, Y., Kakinaga, Y., and Kodaira, T. (2003). Influences of aliphatic alcohols on crystallization of large mordenite crystals and their sorption properties. **Journal of Materials Chemistry**. 13: 181–185.
- Sadeghbeigi, R. (2012). Fluid Catalytic Cracking Handbook - Chapter 4 FCC Catalysts. **Elsevier Inc., Amsterdam**.
- Sano, T., Wakabayashi, S., Oumi, Y., and Uozumi, T. (2001). Synthesis of large mordenite crystals in the presence of aliphatic alcohol. **Microporous and Mesoporous Materials**. 46: 67–74.
- Shanbhag, G. V., Choi, M., Kim, J., and Ryoo, R. (2009). Mesoporous sodalite: A novel, stable solid catalyst for base-catalyzed organic transformations. **Journal of Catalysis**. 264: 88–92.
- Sharma, P., Yeo, J. gu, Yu, J. haeng, Han, M. H., and Cho, C. H. (2014). Effect of ethanol as an additive on the morphology and crystallinity of LTA zeolite. **Journal of the Taiwan Institute of Chemical Engineers**. 45: 689–704.
- Tekin, R., Bac, N., Warzywoda, J., and Sacco, A. (2015). Encapsulation of a fragrance molecule in zeolite X. **Microporous and Mesoporous Materials**. 215: 51–57.
- Uguina, M. A., de Lucas, A., Ruiz, F., and Serrano, D. P. (1995). Synthesis of ZSM-5 from ethanol-containing systems. Influence of the gel composition. **Industrial and Engineering Chemistry Research**. 34: 451–456.

- Yang, X., and Albrecht, D. (2006). Revision of Charnell ' s procedure towards the synthesis of large and uniform crystals of zeolites A and X. **Microporous and Mesoporous Materials**. 90: 53–61.
- Yao, J., Zhang, L., and Wang, H. (2008). Synthesis of nanocrystalline sodalite with organic additives. **Materials Letters**. 62: 4028–4030.



CHAPTER II

LITERATURE REVIEW

This chapter provides the literature review of structures and applications of zeolites including zeolite X, EMT/FAU intergrowth, and nanosized SOD zeolites. The effect of ethanol on zeolite phase and morphology is summarized. Finally, the literature about the synthesis methods of the zeolites involved in this work as well as their drawbacks are reviewed.

2.1 Background of zeolite

2.1.1 Zeolite structure

Zeolite is a crystalline aluminosilicate material. It is classified in a microporous class with the unique and well-defined pore sizes and channels. Zeolite structure is formed by Primary Building Units (PBUs), SiO_4 and AlO_4 tetrahedra, sharing oxygen atoms, as shown in Figure 2.1 (Guo, 2016). The negative charges from the presence of the AlO_4 units are typically balanced by sodium or potassium cations from precursors that can be easily exchanged by other cations (Frising et al., 2008). The PBUs combine by sharing oxygen atom with adjacent tetrahedra to form Secondary Building Units (SBUs). Figure 2.2 shows that the SBUs including 6-membered ring ($6mr$) and 4-membered ring ($4mr$) are connected together to form composite building units (CBUs). The CBUs are linked to other components to form unique zeolite

structures. The different orientations of the CBUs also build up the different framework types of zeolite (Lui, 2014). Nowadays, types of zeolite reported by the International Zeolite Association (IZA) include more than 240 framework types.

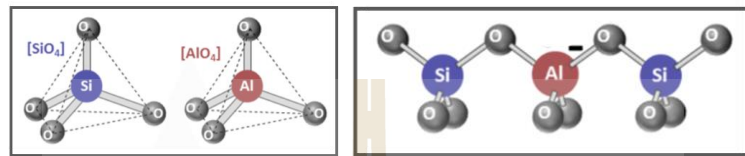


Figure 2.1 Left: SiO₄ and AlO₄ tetrahedra, Primary Building Units (PBUs) of zeolite Right: The negative charges of the AlO₄ units are formed by structure linkage of PBUs (adapted from Guo, 2016).

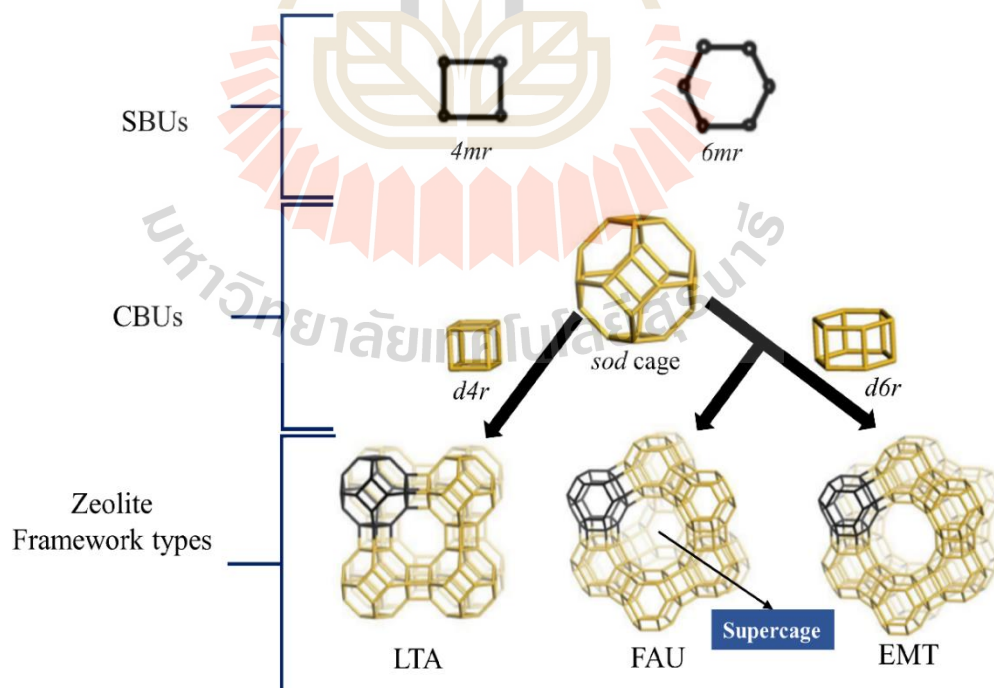


Figure 2.2 Different framework types of zeolite created by the different SBUs and CBUs, and orientations of CBUs (adapted from (Lui, 2014)).

2.1.2 Zeolite X (FAU-type)

In crystallography, FAU framework is classified into the cubic crystal system with $a = 24.74 \text{ \AA}$. In more detail, the FAU framework type composes of *d6r* units and *sod* cages. Each *sod* cage links with four *d6r* units, while every *d6r* unit connects with two *sod* cages, causing formation of three-dimensional pore and channel system. Zeolite X with the 12-membered-ring pore openings in the center of the FAU structure, called supercage with a pore size of 7.4 \AA , is categorized into large pore zeolites, as shown in Figure 2.2.

The elemental composition of hydrated FAU unit cell can be indicated as $[M_a(H_2O)_b][Al_aSi_{192-a}O_{384}]$, where a represents number of Al atom per unit cell, b is number of water molecules and M stands for monovalent cation (or one-half of divalent). The value range of “ a ” can vary from 96 to less than 4, implying that Si/Al ratios is 1 to more than 50. However, zeolite X contains 77-96 Al atoms, referring to Si/Al ratios between 1 and 1.5 (Kulprathipanja, 2010).

Zeolite X is widely used in many industries because of its high surface area, large void volume and pore openings in a three-dimensional channel system, high stability, crystallinity and well-defined porous structure. Moreover, zeolite X with high ion-exchange capacity, resulting from low Si/Al ratio, is utilized as an ion exchanger and adsorbent (Julbe et al., 2015). For examples, the shape- and size- selectivity of zeolite X pores is utilized in encapsulation application. Tekin et al. (2015) encapsulated a fragrance molecule, triplal, in zeolite X with different crystallize sizes. Additionally, Tekin et al. (2016) prepared Zn^{2+} and Cu^{2+} ion-exchange zeolite X containing fragrance molecules for antimicrobials which show excellent antimicrobial activities against

microorganism. In addition, zeolite X with high surface area is normally used as a supports of Cu active species for decarboxylative coupling reaction of cinnamic acids and alcohols and oxidative coupling reaction of alkenes and aldehydes (Chen et al., 2016), and of potassium catalyst for transesterification reaction of Jatropha seed oil (Manadee et al., 2017).

2.1.3 Intergrowth of EMT/FAU zeolite

The FAU zeolite is widely used in catalytic applications, due to its large pore size with four 12-member ring pore openings (0.74 nm) and thermal stability. In crystallography, the FAU zeolite is classified in space group Fd3m, a cubic unit cell. Its structure is built up from stacking sodalite layers in an ABCABC sequence, which is related by a center of inversion in the double six-member rings (Van Bekkum et al., 2001).

The EMT zeolite is in space group P63/mmc, a hexagonal unit cell. Its structure comprises of the stacking of sodalite layers in a ABAB sequence, which has a reflection relationship between neighbouring layers. The EMT zeolite contains two types of supercages, including hypocage (0.5 nm³) with three 12-member ring pore openings (Derouane et al., 1991) and hypercage (1.3 nm³) with five 12-member ring pore openings (Thomas et al., 1981).

The EMT/FAU intergrowth is formed by changing symmetry elements, reflection or center of inversion, of sodalite layers between neighbouring sheets, as shown in Figure 2.3. It means that this solid contains both cubic and hexagonal sheets, and three types of pores, including hyper- and hypocages of EMT zeolite and supercage of FAU zeolite.

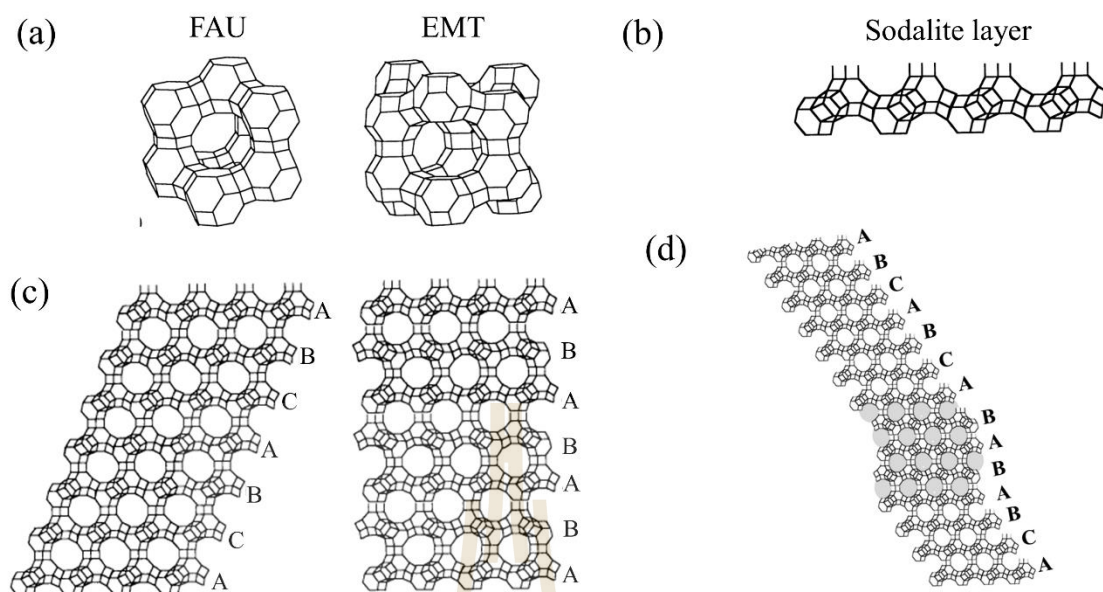


Figure 2.3 (a) Structure of FAU and EMT zeolites, (b) sodalite layer, (c) different orientations of sodalite cages in FAU (ABABAB...) and EMT (ABCABCABC...), and (d) the random stacking of sodalite layer in EMT/FAU intergrowth.

The intergrowth of FAU/EMT zeolite comprises of the FAU and EMT layers in the same bulk structure, resulting in a combination of advantages of both zeolites. Consequently, this zeolite is normally used as a catalyst support. Belandría et al. (2008) used the EMT/FAU zeolite as support of Pt catalyst for an n-pentane hydroisomerization reaction. The catalytic performance of the catalysts decreased in the following order: Pt/EMT/FAU > Pt/EMT > Pt/FAU (Belandría et al., 2008). Additionally, Gao et al. (2015) prepared the CoMo bimetallic catalyst using the EMT/FAU intergrowth as support. The catalyst exhibited excellent catalytic performance in FCC gasoline hydro-upgrading compared with pure EMT and FAU supports (Gao et al., 2015).

The synthesized methods of the EMT/FAU intergrowth normally takes a long crystallization time, for example, 15 days (Belandría et al., 2008) and 6 days (Gao et al., 2015). The synthesis also requires organic template such as 18-crown-6 and 15-crown-5 (Belandría et al., 2008; Gao et al., 2015).

2.1.4 Nanosized SOD zeolite

Sodalite is SOD-type zeolite with a small pore size of 0.28 nm. The structure is built from *sod* cages which comprise of six *4mr* and eight *6mr* as shown in Figure 2.4 (Khajavi et al., 2007; Eddaoudi et al., 2015). The general chemical composition is $\text{Na}_8[\text{AlSiO}_4]_6(\text{X})_2$, where X stands for a monovalent guest anion.

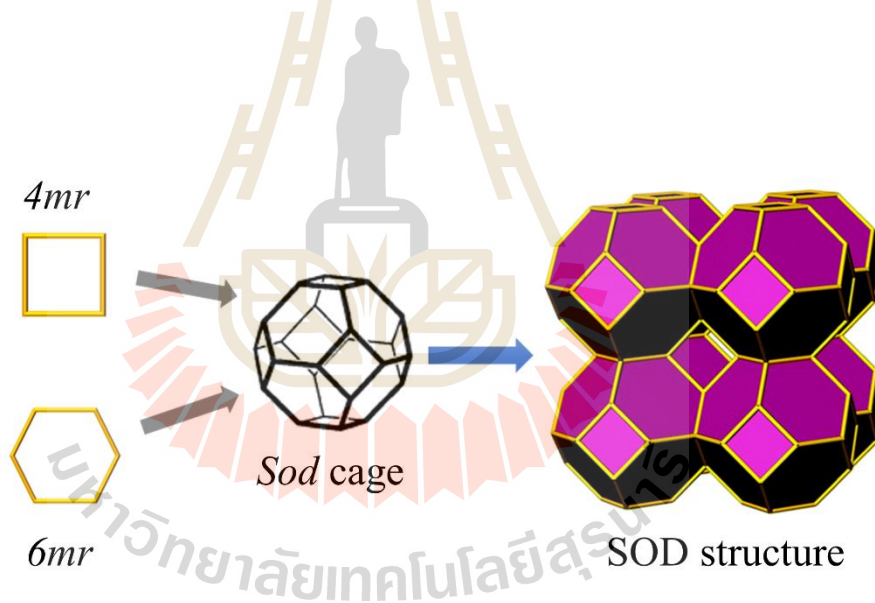


Figure 2.4 SOD structure formed by *sod* cages comprising of six *4mr* and eight *6mr* (adapted from (Khajavi et al., 2007; Eddaoudi et al., 2015).

The sodalite with the small opening-pore size of 0.28 nm, only small molecules, such as helium, ammonia, water and hydrogen, are allowed through the pores of sodalite (Breck, 1974; Nabavi et al., 2014). Consequently, sodalities are

utilized in separation of the small gas molecules from gas or liquid mixtures. They are also used in hydrogen storage and other applications.

Sodalites are rarely applied in catalysis due to the low surface area and small pore size, which lead to low number of active sites and limit molecular diffusion, respectively. However, sodalites with high surface areas, such as mesoporous sodalite and nano-sized crystals have potential in catalysis as support or catalyst. For examples, Shanbhag et al. (2009) synthesized mesoporous sodalite with a surface area of $193 \text{ m}^2/\text{g}$ and pore volume of $0.42 \text{ cm}^3/\text{g}$, about 10- and 4-fold, respectively, larger than the micro-sized sodalite. The mesoporous sodalite in sodium form was ion-exchanged to potassium form and used as a base catalyst for many reactions, including Knoevenagel condensation, Claisen–Schmidt condensation in liquid phase, and acetylacetone cyclization in vapor phase (Shanbhag et al., 2009). The catalyst exhibits higher catalytic performance and has a longer catalyst lifetime than zeolite X in the cesium form and micro-sized sodalite in the potassium form (Shanbhag et al., 2009).

In addition, Kimura et al. (2008) synthesized nano-sized sodalite with diameter around 26 nm and used it as a support for K_2CO_3 . This catalyst exhibits a high activity in oxidation of carbon. Hiyoshi et al. (2012) synthesized nano-sized sodalite with an average crystallite diameter of 47 nm and large surface area of $73 \text{ m}^2/\text{g}$. The nanosized sodalite is used as catalyst for epoxidation of 2-cyclohexen-1-one with hydrogen peroxide. The catalyst provided a high conversion of up to 90% at a reaction time of 100 min. It was easily recovered after the reaction by filtration and re-used four times after regeneration with a slight decrease in the performance (Hiyoshi et al., 2012).

There are several reports about the synthesis of nanosized SOD zeolite as shown in Table 2.1. Yao et al. (2006) synthesized sodalite nanocrystals by direct transformation of nanocrystals of sodalite in a basic solution. Li et al. (2007) synthesized organic-functionalized sodalite nanocrystals with a short crystallization time. However, the overall time of both processes is about 4 days (Yao et al., 2006) and 15 days (Li et al., 2007) due to the long preparation of colloidal silicalite nanocrystals encapsulated by tetrapropylammonium hydroxide (TPAOH). Moreover, TPAOH is expensive resulting in high synthesis cost. To reduce the cost of the synthetic process, a template-free method is preferred. Hiyoshi (2012) successfully synthesized nanosized sodalite from template-free reaction gels in a basic condition.

The conventional synthesis methods of both EMT/FAU intergrowth and nanosized SOD zeolite requires a long crystallization time and high crystallization temperature that result in a long process and high energy consumption. Moreover, the use of organic templates requires calcination process for removal which also consumes more energy and produces organic wastes. So, it is worthwhile to develop a template-free method with a short crystallization time and low crystallization temperature.

Table 2.1 Synthesis of nanosized SOD zeolite from various condensation reactions in basic solution.

Starting reagents	Crystallization condition	Particle size (nm)	Surface area (m ² /g)	Reference
Silicalites encapsulated by				
TPAOH + NaAlO ₂ + NaOH + H ₂ O	80 °C, 3 h	40-110	NR	(Yao et al., 2006)
Silicalites encapsulated by				
TPAOH + NaAlO ₂ + NaOH + H ₂ O	80 °C, 3-4 h	60-140	19.1-22.8	(Li et al., 2007)
Na ₂ SiO ₃ ·9H ₂ O + NaAlO ₂ + NaCl + H ₂ O	150 °C, 42 h	47-48	65-73	(Hiyoshi, 2012)

NR = not reported

TPAOH: Tetrapropylammonium hydroxide

2.2 Effect of ethanol on zeolite synthesis

Ethanol is normally used as an organic solvent in organic synthesis. Several researchers have successfully synthesized various zeolites from ethanol-containing gels including (Uguina et al., 1995; Sano et al., 2001; Oumi et al., 2003; Yao et al., 2008; Huang et al., 2011; Sharma et al., 2014; Chen et al., 2018). The presence of ethanol in synthesis gels of the zeolites directly affects the properties of the gel including gel density, pH and Na⁺ concentrations (Huang et al., 2011) that influence the crystallization process. However, effect of ethanol on the phase and morphology of zeolite depends on the gel composition and the amount of added ethanol.

Up to now, many researchers reported that ethanol affects only the zeolite morphology. For examples, Uguina et al. (1995) synthesized the ZSM-5 with high crystallinity. Ethanol accelerates both the nucleation rate and the crystal growth rate in the zeolite crystallization process. Moreover, the ethanol affects the crystallite size but not the Si/Al ratio of the products. Sano et al. (2001) and Oumi et al. (2003) synthesized the pure, uniform and large crystals of mordenite in the presence of the aliphatic alcohol system including ethanol. These studies have revealed that ethanol might have a buffering effect on the crystal growth, resulting in slow release of reactive species, and affected only the zeolite morphology but not the zeolite phase. Additionally, Zhang et al. (2018) reported that adding ethanol in one-pot reaction gels affects zeolite Y morphology. The presence of ethanol in the reaction mixtures induces the change of the morphology of the NaY zeolite crystals from the submicron octahedral shape, a typical morphology of the zeolite Y, to micron-sized microspheres (MFAU). They also found that alkyl and hydroxyl groups play the important roles on crystal surface interactions. Alkyl group of alcohol could interact with the crystal surface vacancies, whereas hydroxyl group could create hydrogen bond with silanol groups on the crystal surface, resulting in multi facet crystals. The alkyl chain creates a hydrophobic interaction with the crystal surfaces which is a large steric hindrance to hinder bulk nutrient, resulting in the change of zeolite Y morphology (Chen et al., 2018).

In addition, the difference of ethanol contents in the gel can affect both final zeolite phase and morphology. Yao et al. (2003) synthesized nanosized sodalite from zeolite A gel with organic additives including ethanol. They found that ethanol slowed down zeolite crystallization process resulting in the formation of the nanosized sodalite and also affected phase of the resulting zeolites. In similar study, Huang et al. (2011)

reported that the various amounts of ethanol content in the reaction gel significantly affect the final phase and morphology of the zeolite. The hollow sodalite structures, are successfully synthesized in the synthesis gel of LTA zeolite containing ethanol. Additionally, LTA zeolite is produced at low ethanol contents, whereas SOD zeolite is preferred at high ethanol contents. They also proposed the formation mechanism of zeolite in this system that starts with the creation of amorphous spherical particles, multinucleation and growth of shell nanocrystals, and digestion of the amorphous core. Moreover, addition of ethanol in the reaction gel slows down crystallization rate of zeolite, rendering small crystal sizes, and changes the physical properties of the gel, such as density and pressure. When the amount of ethanol is increased, the gel is denser as observed by the partition of solution into two phases, resulting in more concentrated gel. This phenomenon enhances the degree of supersaturation of the gel phase, increases the nucleation rate, and accelerates an aggregation of materials, affecting the zeolite phase and morphology.

It is more complicated and still unclear about the effect of ethanol at the molecular scale. However, researchers have reported that the interfaces of the water clathrate framework formed around the cation during hydrophobic hydration are surrounded by ethanol molecule (Franks et al., 1966; Dixit et al., 2002). They have also proposed that one of the factors affecting in zeolite growth is the interchange of the clathrate water molecules and reactive aluminosilicate species. When mass transport rate is reduced by the strong interaction between ethanol and water molecules might be slow exchange rate of solvated reactive aluminosilicate species and clathrate water molecules around the cation, resulting in decrease a zeolite growth rate.

2.3 Strategy to develop the synthesis methods of EMT/FAU intergrowth and nanosized SOD zeolite

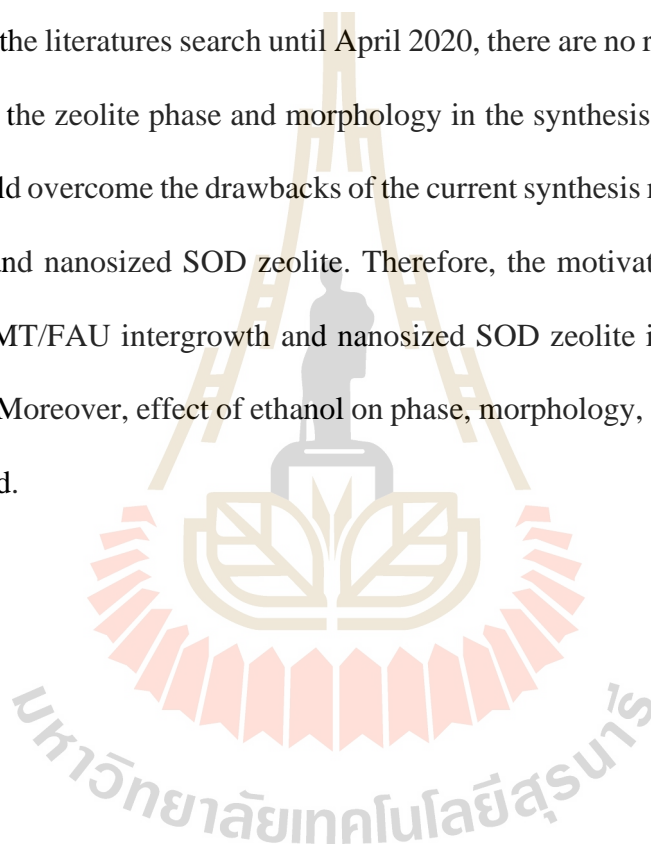
To overcome the drawbacks of the current synthesis methods of EMT/FAU intergrowth and nanosized SOD zeolite, the synthesis method of zeolite NaX in the literature (Mintova et al., 2016) is interesting. Zeolite X can be synthesized in one-pot synthesis of sodium aluminate and sodium silicate in a base solution. Moreover, this method is template-free with 18 h to complete crystallization process. The short crystallization time could save cost and energy consumption compared with the synthesis methods of the EMT/FAU intergrowth and nanosized SOD zeolite. Moreover, there are reports that other zeolite phases are produced in the synthesis of the zeolite X, for example, LTA (Ansari et al., 2014; Maatoug et al., 2017), EMT/FAU intergrowth (Gao et al., 2015), SOD (Hums, 2017) and GIS (Dhainaut et al., 2013; Hums et al., 2015; Musyoka et al., 2015; Maatoug et al., 2017).

The information from the literatures means that the EMT/FAU intergrowth and SOD zeolites could be synthesized from the synthesis gel of zeolite X by modifying parameters such as heating method, time, temperature, concentrations of reactants and additives. Among several parameters, the addition of additive in the synthesis gel is simple and interesting. The presence of ethanol in the gels directly affects the gel properties including density, pH and Na⁺ concentration that influence the crystallization process, morphology, and phase of the zeolite (Huang et al., 2011).

Up to April 2020, there are not many reports about the synthesis of EMT/FAU intergrowth and nanosized SOD in ethanol-containing system. Ethanol has potential to act as an additive in the synthesis of the EMT/FAU intergrowth and nanosized SOD

zeolite from the zeolite X gel. Huang et al. (2011) synthesized hollow nanosized SOD zeolite with controllable size and morphology from the gel of LTA-type zeolite in ethanol-water system. They revealed that ethanol accelerates phase transformation of other phases to SOD zeolite. In addition, Gao et al. (2015) synthesized the EMT/FAU intergrowth by increasing sodium oxide content in the synthesized gel of FAU zeolite.

From the literatures search until April 2020, there are no reports about the effect of ethanol on the zeolite phase and morphology in the synthesis of the zeolite X. This approach could overcome the drawbacks of the current synthesis methods of EMT/FAU intergrowth and nanosized SOD zeolite. Therefore, the motivation of this work is to synthesize EMT/FAU intergrowth and nanosized SOD zeolite in the synthesis gel of zeolite NaX. Moreover, effect of ethanol on phase, morphology, and porosity of zeolite is investigated.



2.4 References

- Ansari, M., Aroujalian, A., Raisi, A., Dabir, B., and Fathizadeh, M. (2014). Preparation and characterization of nano-NaX zeolite by microwave assisted hydrothermal method. **Advanced Powder Technology**. 25: 722–727.
- Belandría, L. N., González, C. S., Aguirre, F., Sosa, E., Uzcátegui, A., González, G., Brito, J., González-Cortés, S. L., and Imbert, F. E. (2008). Synthesis, characterization of FAU/EMT intergrowths and its catalytic performance in n-pentane hydroisomerization reaction. **Journal of Molecular Catalysis A: Chemical**. 281: 164–172.
- Breck, D. W. (1974). Zeolite molecular sieves, **John Wiley & Sons Inc., New York**.
- Chen, S., Shao, Z., Fang, Z., Chen, Q., Tang, T., Fu, W., Zhang, L., and Tang, T. (2016). Design and synthesis of the basic Cu-doped zeolite X catalyst with high activity in oxidative coupling reactions. **Journal of Catalysis**. 338: 38–46.
- Chen, Z., Chen, C., Zhang, J., Zheng, G., Wang, Y., Dong, L., Qian, W., Bai, S., and Hong, M. (2018). Zeolite Y microspheres with perpendicular mesochannels and metal@Y heterostructures for catalytic and SERS applications. **Journal of Material Chemistry A**. 6: 6273–6281.
- Derouane, E. G., Lemos, F., Naccache, C., and Ramôa Ribeiro, F. (Eds.) (1991). Zeolite Microporous Solids: Synthesis, Structure, and Reactivity. **Springer, Heidelberg**.
- Dhainaut, J., Daou, T. J., Chappaz, A., Bats, N., Harbuzaru, B., Lapisardi, G., and Chaumeil, H. (2013). Synthesis of FAU and EMT-type zeolites using structure-directing agents specifically designed by molecular modelling. **Microporous and Mesoporous Materials**. 174: 117–125.

- Dixit, S., Crain, J., Poon, and W. C. K. (2002). Molecular segregation observed in a concentrated alcohol – water solution. **Nature**. 416: 829–832.
- Hums E. (2017). Synthesis of Phase-Pure Zeolite Sodalite from Clear Solution Extracted from Coal Fly Ash. **Journal of Thermodynamics & Catalysis**. 08: 1–6.
- Eddaoudi, M., Sava, D. F., Eubank, J. F., Adil, K., and Guillermin, V. (2015). Zeolite-like metal-organic frameworks (ZMOFs): Design, synthesis, and properties. **Chemical Society Reviews**. 44: 228–249.
- Franks, F., and Ives, D. J. G. (1966). The structural properties of alcohol-water mixtures. **Quarterly Reviews Chemical Society**. 20: 1–44.
- Frasing, T., and Leflaive, P. (2008). Extraframework cation distributions in X and Y faujasite zeolites: A review. **Microporous and Mesoporous Materials**. 114: 27–63.
- Gao, D., Duan, A., Zhang, X., Zhao, Z., Hong, E., Qin, Y., and Xu, C. (2015). Synthesis of CoMo catalysts supported on EMT / FAU intergrowth zeolites with different morphologies and their hydro-upgrading performances for FCC gasoline. **Chemical Engineering Journal**. 270: 176–186.
- Hiyoshi, N. (2012). Nanocrystalline sodalite: Preparation and application to epoxidation of 2-cyclohexen-1-one with hydrogen peroxide. **Applied Catalysis A: General**. 419–420: 164–169.
- Huang, Y., Yao, J., Zhang, X., Kong, C., Chen, H., Liu, D., Tsapatsis, M., Hill, M. R., Hill, A. J., and Wang, H. (2011). Role of ethanol in sodalite crystallization in an ethanol-Na₂O-Al₂O₃-SiO₂-H₂O system. **CrystEngComm**. 13: 4714–4722.

- Hums, E., Musyoka, N. M., Baser, H., Inayat, A., and Schwieger, W. (2015). In-situ ultrasound study of the kinetics of formation of zeolites Na-A and Na-X from coal fly ash. **Research on Chemical Intermediates**. 41: 4311–4326.
- Julbe, A., and Drobek, M. (2015). Zeolite X: Type. In: Drioli, E. & L. Giorno (eds.), **Encyclopedia of Membranes**. Springer, Heidelberg.
- Khajavi, S., Kapteijn, F., and Jansen, J. C. (2007). Synthesis of thin defect-free hydroxy sodalite membranes: New candidate for activated water permeation. **Journal of Membrane Science**. 299: 63–72.
- Kulprathipanja, S. (2010). **Zeolites in Industrial Separation and Catalysis**, Wiley-VCH Verlag GmbH, Weinheim.
- Li, D., Yao, J., Wang, H., Hao, N., Zhao, D., Ratinac, K. R., and Ringer, S. P. (2007). Organic-functionalized sodalite nanocrystals and their dispersion in solvents. **Microporous and Mesoporous Materials**. 106: 262–267.
- Lui, L. (2014). **Inorganic and metal-organic framework materials (PhD's dissertation)**. Stockholm University, Sweden.
- Maatoug, N., Delahay, G., and Tounsi, H. (2017). Valorization of vitreous China waste to EMT / FAU, FAU and Na-P zeotype materials. **Waste Management**. 74: 267–278.
- Manadee, S., Sophiphun, O., Osakoo, N., Supamathanon, N., Kidkhunthod, P., Chanlek, N., Wittayakhun, J., and Prayoonpokarach, S. (2017). Identification of potassium phase in catalysts supported on zeolite NaX and performance in transesterification of Jatropha seed oil. **Fuel Processing Technology**. 156: 62–67.

Mintova, S., and Barrier, N. (2016). Verified syntheses of zeolitic materials.

Commission of the international zeolite association.

Musyoka, N. M., Petrik, L. F., Hums, E., Kuhnt, A., and Schwieger, W. (2015).

Thermal stability studies of zeolites A and X synthesized from South African coal fly ash. **Research on Chemical Intermediates**. 41: 575–582.

Nabavi, M. S., Mohammadi, T., and Kazemimoghadam, M. (2014). Hydrothermal

synthesis of hydroxy sodalite zeolite membrane: Separation of H₂/CH₄.

Ceramics International. 40: 5889–5896.

Oumi, Y., Kakinaga, Y., and Kodaira, T. (2003). Influences of aliphatic alcohols on

crystallization of large mordenite crystals and their sorption properties.

Journal of Material Chemistry. 13: 181–185.

Sano, T., Wakabayashi, S., Oumi, Y., and Uozumi, T. (2001). Synthesis of large

mordenite crystals in the presence of aliphatic alcohol. **Microporous and**

Mesoporous Materials. 46: 67–74.

Shanbhag, G. V., Choi, M., Kim, J., and Ryoo, R. (2009). Mesoporous sodalite: A

novel, stable solid catalyst for base-catalyzed organic transformations.

Journal of Catalysis. 264: 88–92.

Sharma, P., Yeo, J. gu, Yu, J. haeng, Han, M. H., and Cho, C. H. (2014). Effect of

ethanol as an additive on the morphology and crystallinity of LTA zeolite.

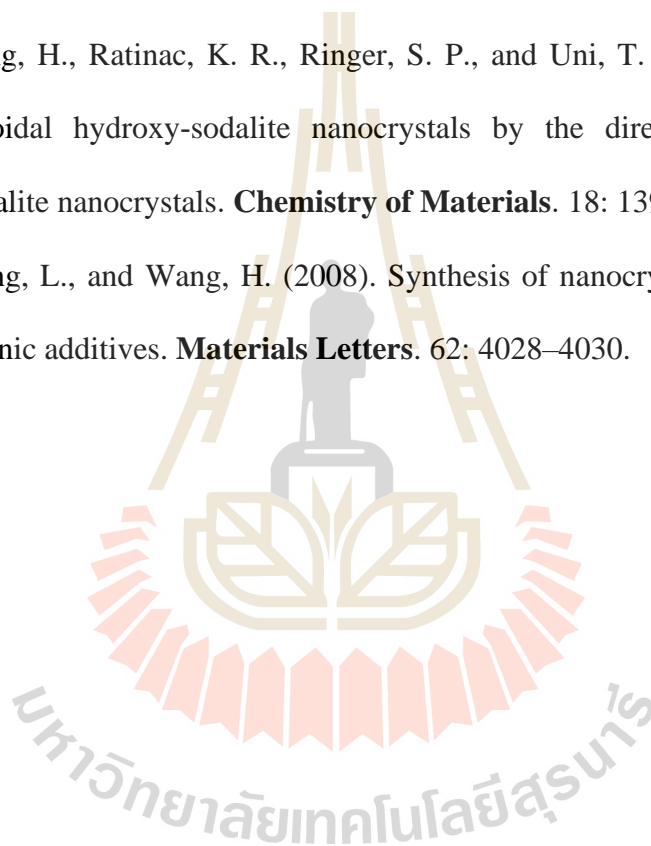
Journal of the Taiwan Institute of Chemical Engineers. 45: 689–704.

Thomas, J. M., Audier, M., and Klinowski, J. (1981). A new family of crystalline, three

dimensionally ordered, microporous structures. **Journal of the Chemical**

Society, Chemical Communications. 843: 1221–1222.

- Uguina, M. A., de Lucas, A., Ruiz, F., and Serrano, D. P. (1995). Synthesis of ZSM-5 from Ethanol-Containing Systems. Influence of the Gel Composition. **Industrial and Engineering Chemistry Research**. 34: 451–456.
- Van Bekkum, H., Flanigen, E. M., Jacobs, P. A., and Jansen, J. C. (2001). Introduction to Zeolite Science and Practice., Studies in Surface Science and Catalysis. **Elsevier, Amsterdam**
- Yao, J., Wang, H., Ratinac, K. R., Ringer, S. P., and Uni, T. (2006). Formation of colloidal hydroxy-sodalite nanocrystals by the direct transformation of silicalite nanocrystals. **Chemistry of Materials**. 18: 1394–1396.
- Yao, J., Zhang, L., and Wang, H. (2008). Synthesis of nanocrystalline sodalite with organic additives. **Materials Letters**. 62: 4028–4030.



CHAPTER III

EXPERIMENTAL

3.1 Chemicals

Chemicals used in this research are listed in Table 3.1.

Table 3.1 Chemicals used in this research.

Chemicals	Formula	Content (%) / grade	Suppliers
Fumed silica	SiO ₂	99%	Carlo Erba
Ethanol	CH ₃ CH ₂ OH	95%	LC221200
Sodium hydroxide	NaOH	analytical grade	Carlo Erba
Sodium aluminate	NaAlO ₂	99%	Riedel-de Haën®
Nitric acid	HNO ₃	69%	ANaPURE
Hydrochloric acid	HCl	37%	RCI Labscan
Hydrofluoric acid	HF	49%	QR&C
Boric acid	H ₃ BO ₃	99.5%	Merck
Silicon tetrachloride	SiCl ₄	Certified reference material	Merck
Aluminum nitrate	Al(NO ₃) ₃	Certified reference material	Carlo Erba

3.2 Zeolite synthesis in the ethanol-water system

Zeolite samples were synthesized with a procedure modified from the international zeolite association (IZA) of zeolite X synthesis method (Mintova et al., 2016). A starting gel composition with mole ratio of NaAlO_2 : 4SiO_2 : 16NaOH : $x\text{H}_2\text{O}$: $y\text{Ethanol}$ was prepared with different mole values of water and ethanol (x and y , respectively) as shown in Table 3.2. Sodium silicate solution (14.63 g) as a silicon source was obtained from mixing fumed silica (4.10 g), sodium hydroxide pellet (1.61 g) (NaOH) and deionized (DI) water (8.92 g) together in a 250-mL polypropylene (PP) bottle. The mixture was stirred vigorously for 18 hours to produce a clear solution. Sodium aluminate solution (98.39 g) as an aluminum source was obtained by adding sodium aluminate (1.36 g), sodium hydroxide pellet (9.08 g) into the mixed solvents of DI water and ethanol (87.95 g) in the 250-mL PP bottle and then the mixture was stirred for 1 hour. Then, the sodium silicate (14.63 g) was dropped to the sodium aluminate solutions and further stirred for 1 hour. Finally, the reaction gels were crystallized at 90 °C for 18 hours under a static condition. The resultant products were separated by centrifugation and washed with DI water several times until the measured pH of the supernatant was about 7. After washing, the samples were dried at 110 °C for 24 hours. The obtained samples were designated as EXX where E represents the ethanol and XX stands for the weight of the added ethanol in the synthesized gel. For example, E20 denotes the zeolite prepared by the synthesized gel containing 20 g of the ethanol.

Table 3.2 Gel compositions with different mole of ethanol and water of all samples modified from the starting gel of zeolite NaX.

Sample	Gel composition	Amount of solvents		Molar ratio of ethanol/water
		(grams)		
		Water	Ethanol	
E00	NaAlO ₂ : 4SiO ₂ : 16NaOH: 325.0H ₂ O: 0EtOH	87.94	0	0
E10	NaAlO ₂ : 4SiO ₂ : 16NaOH: 291.6H ₂ O: 13.0EtOH	77.94	10.00	0.045
E20	NaAlO ₂ : 4SiO ₂ : 16NaOH: 258.2H ₂ O: 26.1EtOH	67.94	20.00	0.101
E30	NaAlO ₂ : 4SiO ₂ : 16NaOH: 224.9H ₂ O: 39.1EtOH	57.94	30.00	0.174
E40	NaAlO ₂ : 4SiO ₂ : 16NaOH: 191.5H ₂ O: 52.2EtOH	47.94	40.00	0.273
E50	NaAlO ₂ : 4SiO ₂ : 16NaOH: 158.1H ₂ O: 65.2EtOH	37.94	50.00	0.412
E60	NaAlO ₂ : 4SiO ₂ : 16NaOH: 124.7H ₂ O: 78.3EtOH	27.94	60.00	0.628

3.3 Material characterization

A phase of the obtained products was investigated by X-ray diffraction (XRD) using a Bruker D8 ADVANCE with Cu K α radiation ($\lambda = 1.5418 \text{ \AA}$). About 300 mg of the samples were ground by a mortar and a pestle and filled in a sample holder. The samples were gently pressed by a glass slide to smooth the sample surfaces. The equipment was operated at the voltage of 40 kV and the current of 40 mA. The XRD patterns were collected with an increment of 0.02° at a scan rate of 0.2 s/step. Thermal stability and weight loss of the samples were determined thermogravimetric analysis

(TGA) and differential thermal analysis (DTA) using a Mettler Toledo model TGA/DSC1 in air with a flow rate of 50 mL/min at a heating rate of 10 °C /min. About 10.00 mg of the samples were placed in a pan prior to the analysis. Then, the curves of TGA and DTA were collected in the temperature in range of 35 to 1000 °C. Textural parameters of all samples were analyzed by N₂ adsorption/desorption analysis. About 100 mg of the synthesized zeolites were investigated by a Micromeritics ASAP 2020 at -196 °C (77 K). Prior to the analysis, each sample was degassed at 350 °C under vacuum. The specific surface area and pore volume of the synthesized zeolites were calculated by Brunauer-Emmett-Teller (BET) and Barrett-Joyner-Halenda (BJH) methods, respectively.

Morphology, particle size, Si/Al ratio of the products were investigated by scanning electron microscopy (SEM) with energy-dispersive X-ray spectroscopy (EDX) using JEOL JSM 7800F field-emission scanning electron microscope (FE-SEM). The samples were spread on a carbon tape and coated with gold by sputtering. The fine detail images of the zeolite morphology from transmission electron microscopy (TEM) were taken by Thermo Scientific TALOS F200X operated at 200 kV. Zeolite powders were ground by a mortar and a pestle and suspended in ethanol to form a lightly cloudy suspension. 15 µL of the suspension was dropped on a Cu grid coated by carbon film and dried in a desiccator.

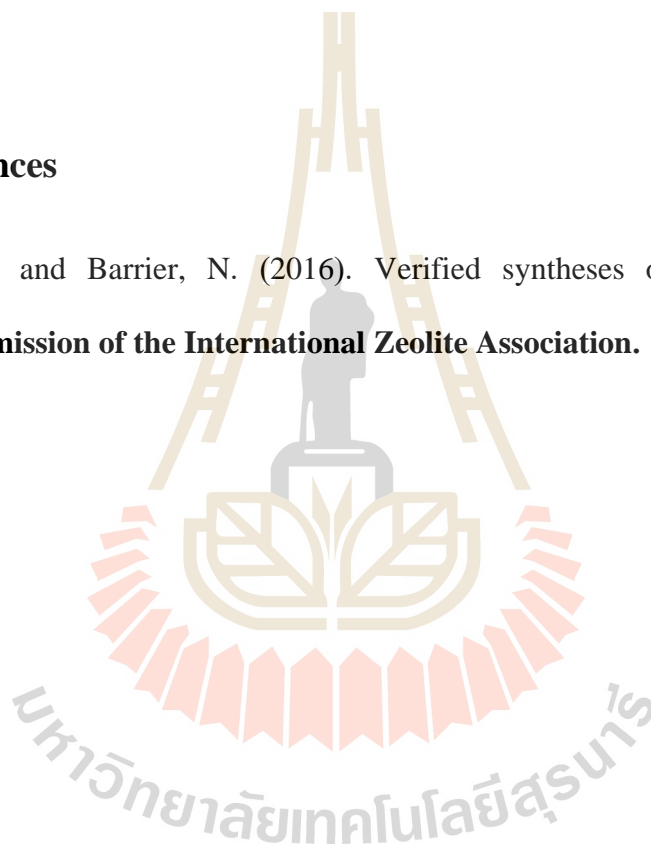
Functional groups of zeolites were analyzed by Fourier-transform infrared spectroscopy (FT-IR) on a Bruker Tensor 27 using attenuated total reflectance (ATR) mode. The zeolite powders were placed on the ATR crystal and firmly pressed by a pressure tower. The sample spectra were collected in a range of 400-350 cm⁻¹ at a

resolution of 4 cm^{-1} for 64 scans. The Si/Al ratio was also determined by an inductively-coupled plasma-optical emission spectrometer (ICP-OES, Perkin Elmer Optima 8000). Each sample was digested in aqua regia, cooled down to room temperature, mixed with boric acid and DI water. The emission wavelengths of silicon and aluminum in solid samples were at 251.611 and 396.153 nm, respectively. The standard solutions were used for the construction of calibration curves for Si and Al.

3.4 References

Mintova, S., and Barrier, N. (2016). Verified syntheses of zeolitic materials.

Commission of the International Zeolite Association.



CHAPTER IV

RESULTS AND DISCUSSION

4.1 Phases of samples from XRD

XRD patterns of all samples shown in Figure 4.1(a). XRD pattern of the E00 which is a general synthesis method of the FAU-type zeolite X without ethanol addition shows only the characteristic peaks of FAU-type zeolite indicated by the filled circle, as expected (Mintova et al., 2016).

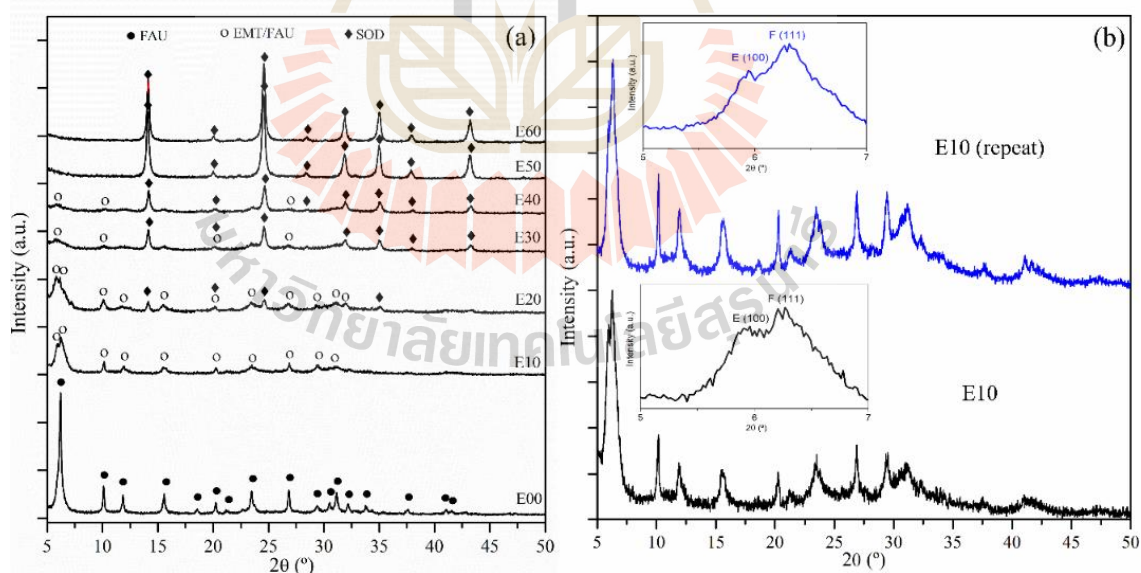


Figure 4.1 XRD patterns of zeolite samples (a) samples prepared from the synthesis gel of NaX with the various ratio of ethanol/water, (b) comparison of the XRD patterns of the E10 from two syntheses at low angle 2theta of 5 to 7 degree.

The XRD pattern of the E10 sample is similar to that of the zeolite X from E00 gel. However, the first peak splits into two peaks at about 5.9 and 6.2 degrees. The split indicates the false or twin stacking of the FAU and EMT layer in the EMT/FAU intergrowth structure (Figure 4.1(b)). Similar observations were reported by Belandría et al. (2008) and Nik et al. (2011). Due to the low solubility of sodium hydroxide in ethanol, the formation of EMT/FAU intergrowth in this system is possible. Since a slight increase of sodium oxide concentration in synthesis gel of FAU zeolite is more favorable for crystallization of the EMT/FAU intergrowth than FAU zeolite, which is consistent with Gao et al. (2015). However, pure EMT zeolite was not observed in any obtained samples. It is possible that the EMT zeolite is the first kinetic and metastable product and it is favored by the low-temperature crystallization temperature and the short crystallization time compared with the FAU and SOD zeolites. Consequently, the long time and high temperature of the zeolite crystallization convert the EMT zeolite to the denser and more stable FAU and SOD zeolites (Ng et al., 2012). The broadening and low intensities of the XRD peaks of this sample is caused by the false or twin stacking of the FAU layer (Treacy et al., 1996), small crystallite size, and low crystallinity. All the causes are due to decrease of crystallization process by ethanol addition (Huang et al., 2011).

To ensure that EMT/FAU intergrowth is reproducible, the synthesis was repeated with the same manner. The XRD pattern of E10(repeat) is compared with the first E10 in Figure 4.1(b). The similar patterns confirm that the EMT/FAU intergrowth could be reproduced in this work.

The XRD patterns of the zeolite powders of E20, E30 and E40 gels show the mixed phases of EMT, FAU and SOD zeolites. The phase of SOD zeolite is observed in the

obtained samples for the first time. Moreover, when the molar ratio of ethanol/water in the synthesis gel was increased, the peak intensity of SOD zeolite increased whereas that of EMT/FAU intergrowth decreased. It is possible that ethanol accelerate the phase transformation of other phases to the SOD zeolite, which is consistent with the reports from Yao et al. (2008) and Huang et al. (2011). However, the EMT/FAU intergrowth can crystallize at these conditions indicating that these zeolites are competitive phases in this system, which is similar to the reports from Gao et al. (2015) and Hums et al. (2017).

With the high molar ratio of ethanol/water in zeolite NaX gel, the XRD patterns of E50 and E60 samples exhibit only characteristic of SOD zeolite with the high peak intensity. The higher ethanol/water ratio results in the larger particle size and higher crystallinity of the SOD zeolite. However, the EMT/FAU intergrowth was not observed anymore at these conditions. It may be that the high ethanol/water ratio in the synthesis gel results in more concentrated gel with higher Na_2O and pH which favors only the SOD crystallization (Huang et al., 2011).

In this system, the phase of the desired zeolite can be controlled by tuning the ratio of ethanol/water in the synthesis gel of zeolite NaX. The ethanol/water molar ratio of 0.045 prefers crystallization of EMT/FAU intergrowth, while the ethanol/water ratios of 0.412 and 0.628 favor crystallization of SOD zeolite

4.2 Vibrational spectra of samples

4.2.1 Vibrational spectra of zeolite structure

The FTIR-ATR spectra of all samples are illustrated in Figure 4.2 to confirm the zeolite structure and to determine the water adsorption capacity of the obtained zeolites. The FT-IR spectrum of the E00 agrees with that of the FAU zeolite from the work of Zhou et al. (2018). The absorption bands at 965 and 1076 cm^{-1} are assigned to the vibration of the asymmetric stretching mode and the tetrahedron of the Si-O bond, respectively. The sharp band at about 455 cm^{-1} is due to internal vibration of the bending mode of the tetrahedral TO_4 ($T = \text{Si}, \text{Al}$), and the band at 565 cm^{-1} is assigned to be double-6-ring (D6R) vibration of the FAU zeolite structure. Moreover, the vibration bands at 751 and 678 cm^{-1} resulting from the external linkage vibrations of the FAU structure are observed, confirming that the FAU zeolite is obtained from this condition.

The spectrum of E10 which is the EMT/FAU intergrowth is the same as that of the FAU zeolite from the E00 sample indicating that the cubic (FAU) and hexagonal (EMT) faujasite cannot be distinguished by the FT-IR spectra. The shift of all vibrational bands of the E10 sample to lower wavenumber compared to the FAU zeolite from E00 gel indicates the lower Si/Al ratio in the skeletal structure of this sample. These observations agree with the work by Lohse et al. (1995).

The spectra of the E50 and E60 are similar to the vibration bands of pure SOD zeolite reported by Huang et al. (2011). The broad band at 965 cm^{-1} is the vibration of the asymmetric stretching mode of the internal T-O-T and the vibration band of the sodalite framework of the SOD zeolite are observed at 425, 460, 666, 703, 727 and 997 cm^{-1} .

In the spectra of the E20, E30 and E40 samples, they are observed in the range of $370\text{-}1250\text{ cm}^{-1}$ which share characteristics of both EMT/FAU intergrowth and SOD zeolite, However, the spectrum feature of the E20 zeolite is closer to that of EMT/FAU intergrowth than the SOD zeolite, while the vibration spectrum of the E40 zeolite is more similar to that of SOD zeolite than that of EMT/FAU intergrowth. Consequently, these results confirm that the higher molar ratio of ethanol/water in the synthesis gel is more favorable crystallization of SOD zeolite than EMT/FAU intergrowth which is consistent with the XRD result.

4.2.2 Water adsorption capacity of the zeolite samples

As shown in Figure 4.2(b), the broad band at 3450 cm^{-1} and the sharp band at 1650 cm^{-1} of all zeolite are assigned to the vibration bands of water in the zeolite structure (Ahmad et al., 2016; Zhou et al., 2018). The intensity of the adsorption bands corresponds to the amount of the chemisorbed water on the zeolite samples. The adsorption bands of the E00 and E10 are larger than those of other samples indicating the high water adsorption capacity of the large pore size FAU and EMT/FAU-type zeolites.

The band intensities of the chemisorbed water of the E50 and E60 samples are lower than those of the other samples because water molecules cannot enter into the small pore of SOD zeolite resulting in low water adsorption. The water adsorption capacity of E20, E30, and E40 directly proportion to the amount of EMT/FAU intergrowth in those samples. However, the difference between the mixed phases of the EMT and FAU zeolites and the intergrowth of the EMT/FAU zeolite cannot be

distinguished by both XRD and FT-IR results. Consequently, the TEM technique was used to investigate this issue.

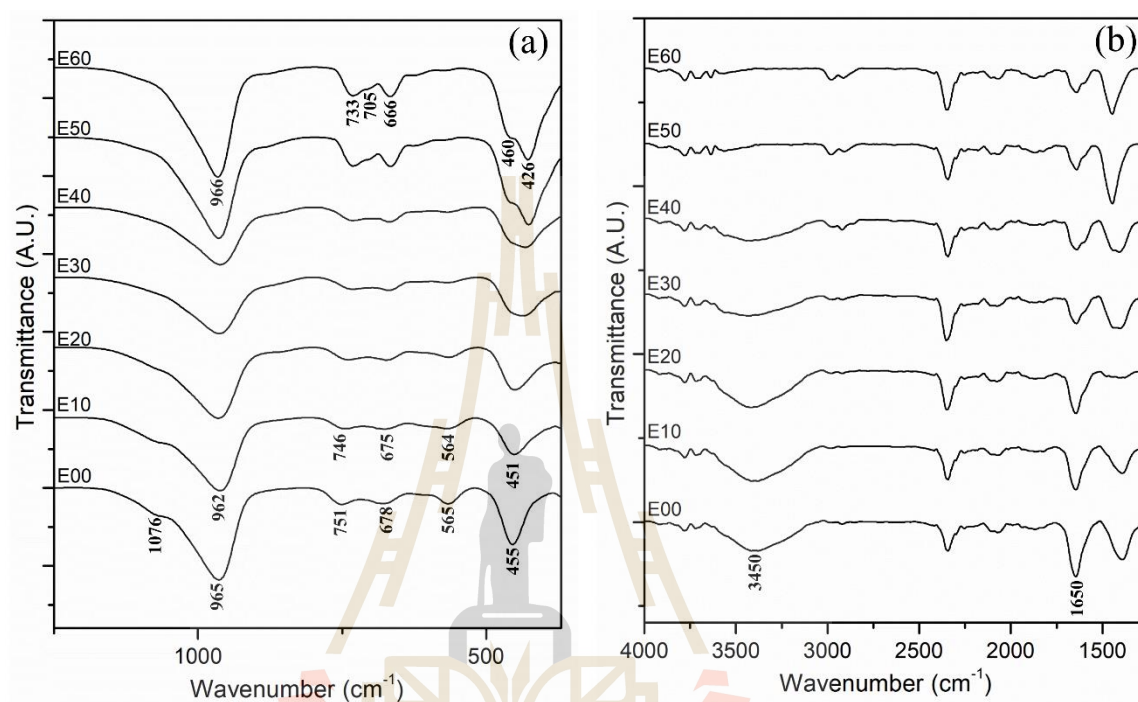


Figure 4.2 FT-IR spectra in the range of (a) 1250-350 cm⁻¹ and (b) 4000-1250 cm⁻¹ of the zeolite samples prepared with different ratios of ethanol/water, E00-E60.

4.3 Morphology of the obtained zeolites from SEM and TEM

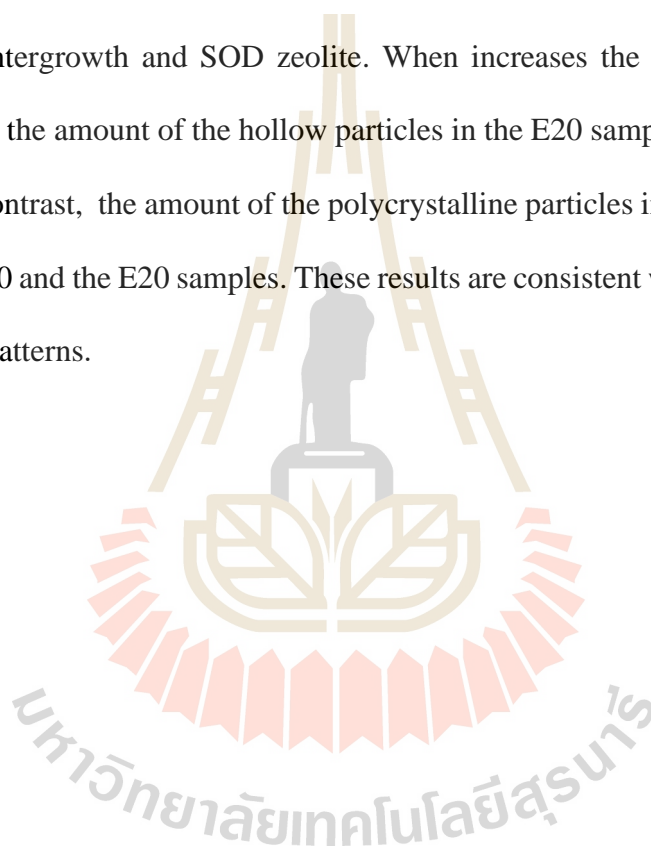
The zeolite products by SEM are shown in Figure 4.3. The morphology of the E00 which is zeolite NaX (Figure 4.3(a)) is cuboctahedral particles with an average size of 1.4 μm . The zeolite particles comprise of hexagonal plate (111) skeleton and nanosheet assemblies with an average thickness of 150 nm. This observation is similar to zeolite morphology reported by Khaleel et al. (2014) and Inayat et al. (2015).

The morphology of the EMT/FAU intergrowth E10 (Figure 4.3(b) and 4.3(c)) are mixtures of perforated hollow and undefined-shape particles. The particles consist of aggregating plate particles with nanosheet on their surfaces, as shown in Figure 4.3(d). These particles share characteristics between the cuboctahedral shape of the FAU zeolite and the hexagonal shape of the EMT zeolite. Moreover, the hollow structure of EMT/FAU intergrowth is expected to be a potential material in catalysis, membrane drug delivery, and material science. Additionally, it has a potential to use as support or catalyst for solving the diffusion limitation of bulky molecules due to the presence of the additional mesopore in the structure (Pagis et al., 2016). Normally, the synthesis methods of this material require templates, such as 18-crown-6 and/or 15-crown-5, and long crystallization time (Belandría et al., 2008; Gao et al., 2015). In this work, the EMT/FAU intergrowth is successfully synthesized by a template-free method in the ethanol-water system with short crystallization time, which helps to reduce cost, energy and hazardous wastes.

As shown in Figure 4.3(h) and 4.3(i), the E50 and E60 morphologies are the agglomerations of polycrystalline SOD particles. The average crystal sizes of that from the E50 and E60 samples are 75 nm and 115 nm, respectively, confirming that nanosized SOD zeolite is obtained. Generally, the SOD zeolite is rarely applied in catalysis due to the small surface area and narrow pore size which leads to low active sites and limit molecular diffusion, respectively. However, the SOD zeolite with large surface such as mesoporous and nanosized SOD zeolite have potential in catalysis as supports and catalysts (Kimura et al., 2008; Shanbhag et al., 2009; Hiyoshi, 2012). Nevertheless, the synthesis methods of those materials required a high crystallization temperature (Shanbhag et al., 2009; Hiyoshi, 2012) or/and organic template (Shanbhag

et al., 2009). In this work, the nanosized SOD zeolite is successfully synthesized by a template-free method with low crystallization temperature which helps to reduce energy and save cost.

Finally, the morphologies of the E20, E30, and E40 samples (Figure 5.3(e) - 5.3(g)). are mixed of polycrystals of the nanosized SOD zeolite and the hollow particles of the EMT/FAU intergrowth as shown in These results confirm the mixed phases of EMT/FAU intergrowth and SOD zeolite. When increases the ethanol/water ratio in synthesis gel, the amount of the hollow particles in the E20 sample is more than that in the E30. In contrast, the amount of the polycrystalline particles in the E40 is more than that of the E30 and the E20 samples. These results are consistent with the zeolite phases in the XRD patterns.



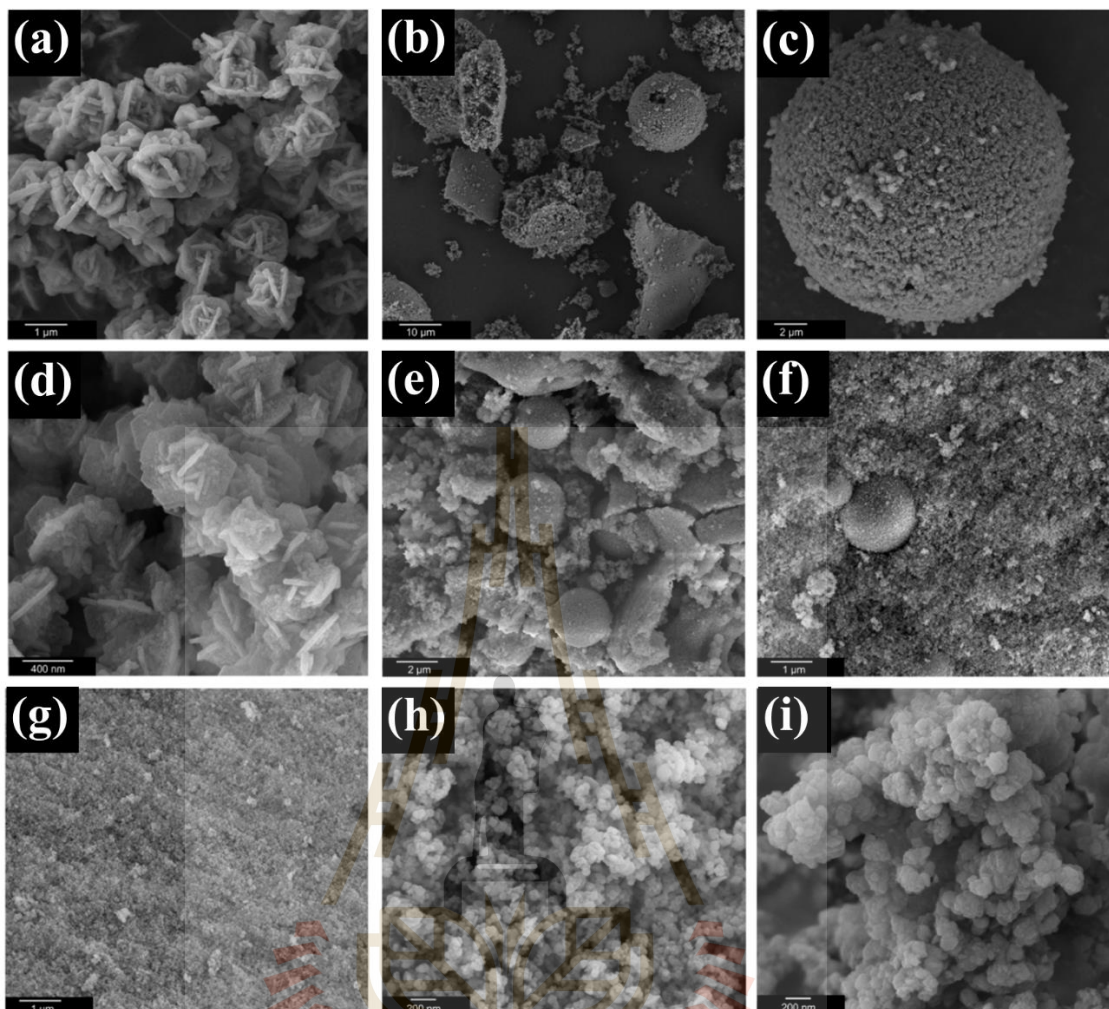


Figure 4.3 SEM images showing morphology of (a) E00, (b)-(d) E10, (e) E20, (f) E30, (g) E40, (h) E50 and (i) E60 samples.

Figure 4.4 shows the TEM images of E00, E10, E50, and E60 samples, which are pure phase zeolites according to the XRD result. The TEM images of the E00 showed that the isolated FAU particles are formed by aggregating the small rod- and plate-like crystals. The degree of the crystal aggregation of the particle core is more than that of the shell area. Each particle is also interconnected by sharing those small

crystals as shown in Figure 4.4(a). Moreover, the agglomeration of the small zeolite crystals is observed as shown in Figure 4.4(b).

Compared to E00, E10 has similar morphology with lower degree of crystal aggregation and less clrae edges. It could imply that the E10 has lower crystallization rate than E00 resulting from ethanol addition. The aggregation of the nanosized crystals on the surfaces of the plate particles is observed in Figure 4.4(c) and 4.4(d). As observed in Figure 4.5, the sample E10 has stacking faults of the EMT and FAU layers in EMT/FAU intergrowth. The observation confirms the EMT/FAU intergrowth is not the mixed phases of the pure EMT and FAU zeolites.

Finally, from Figure 4.4(e) and 4.4(f), the morphology of the SOD zeolite is an aggregation of polycrystalline nanosized SOD zeolite which is consistent with the SEM result.

The results from XRD, SEM, and TEM confirm that the zeolites from the synthesis gel with different ratio of ethanol/water have different phase and morphology. The zeolite formation in this work agrees with the reports from Huang et al. (2011) and Möller et al. (2011). The gel containing ethanol is denser leading to a fast agglomeration and the formation of spherical particles. The spherical particle surface possibly serves as nucleation sites of zeolite. It is possible that numerous nuclei of zeolite quickly grow on the particle shell by consuming amorphous core as a nutrient. As a result, the agglomeration of zeolite particles with hollow structure of EMT/FAU intergrowth and polycrystal of nanosized SOD zeolite is obtained.

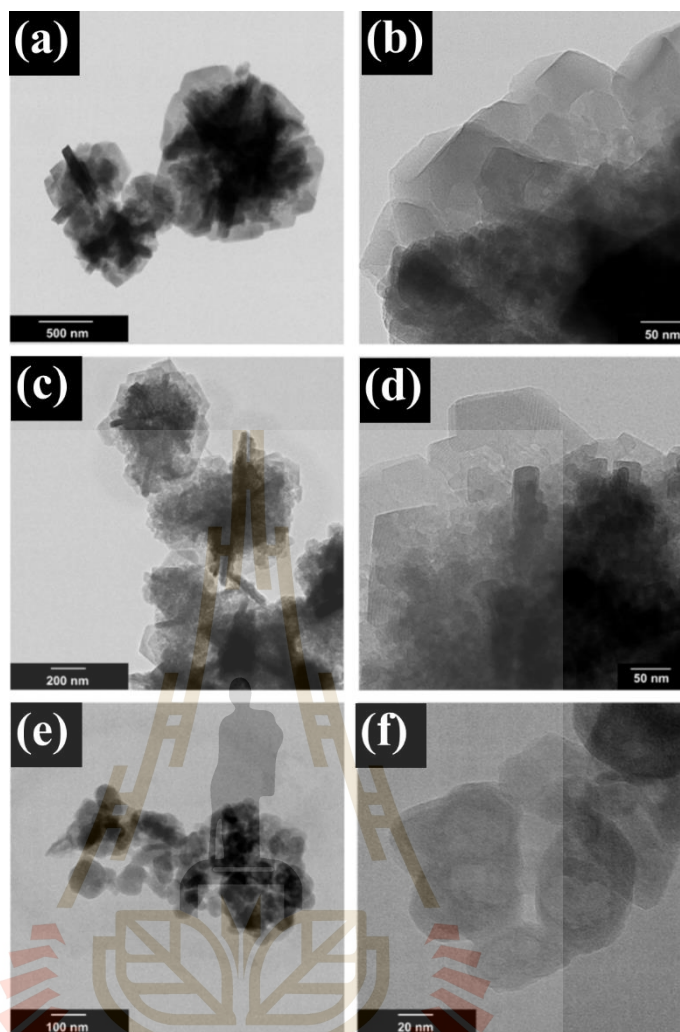


Figure 4.4 Bright-field TEM images of the aggregated zeolite particles of (a) and (b) FAU zeolite from E00, (c) to (e) EMT/FAU intergrowth from E10 and (e) and (f) SOD zeolite from E50.

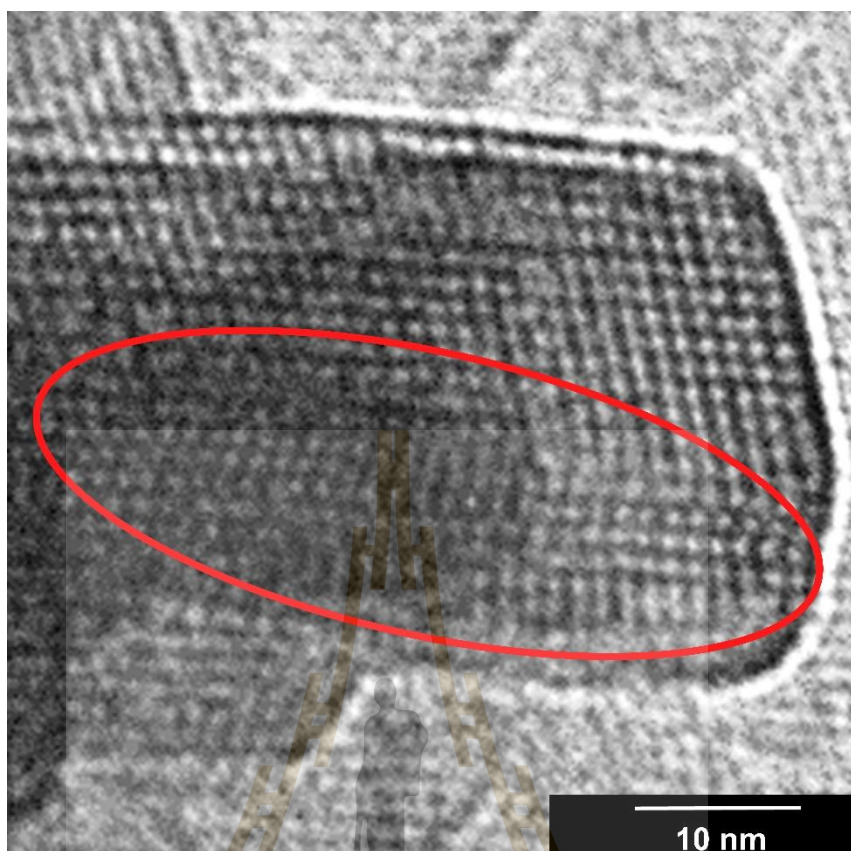


Figure 4.5 Bright-field TEM images of the EMT-FAU intergrowth synthesized from the E10 gel showing the stacking fault of the EMT and FAU layers as shown in the red oval area.

4.4 Isotherms, pore size distributions, textural parameters, and Si/Al ratio of the synthesis materials

The nitrogen adsorption-desorption isotherms and pore size distributions of the synthesis materials are exhibited in Figures 4.6 and 4.7, respectively. Their textural parameters and Si/Al ratio are shown in Table 4.1. The adsorbed volume from E00 increases sharply at low pressure and becomes constant as shown in Figure 4.6(a). This is the characteristic of type I(a) isotherm which is the adsorption in micropores of

zeolite. From E10, the adsorbed volume is lower than that of E00. The isotherm also contains a hysteresis loop. This behavior could be attributed to the lower crystallinity of the EMT/FAU intergrowth. The pore size distribution of the E10 exhibits an average size of 6.7 nm as shown in Figure 4.7(b). The E00 and E10 have high BET surface area and the pore volume of due to large pore size of the FAU zeolite and the EMT/FAU intergrowth.

As shown in Figure 4.6(c), the isotherms of the E50 and E60 samples are type III which is typical of nonporous material because nitrogen molecules cannot enter into the small pore size of the SOD zeolite which causes low surface area and pore volume of micropore in SOD zeolite. The isotherm features of these samples also consist of hysteresis loops at high pressure which is the behavior of nanosized zeolite (Mintova et al., 2015). The size of the hysteresis loop of E60 is smaller than that of E50 due to the larger crystal size. Since E60 was synthesized from the gel with higher ethanol content, this result confirms that ethanol accelerates the crystallization of the SOD zeolite. These results are consistent with the literature that the surface area nanosized SOD is higher than the micro-sized SOD (Hiyoshi, 2012).

As shown in Figure 4.6(b), the isotherms of the E20, E30, and E40 samples share the characteristics of the EMT/FAU intergrowth and the SOD zeolite as shown. The SOD does not adsorb nitrogen because its pore size is smaller than the size of the nitrogen molecule. Thus, the decrease of the EMT/FAU phase and the increase of SOD phase result in less adsorbed volume and, consequently, smaller BET surface area. Moreover, the hysteresis loops at high pressure might be attributed to aggregates and hollow particles of EMT/FAU and polycrystal of SOD.

Figure 4.7 shows an interesting point. All obtained zeolites have external surface and mesoporous volume in their structure which may help to prevent the catalyst deactivation due to the diffusion limitation of the bulky molecules in catalysis. The mesopores are from the aggregation of small or nanosized zeolite crystals to build up the intercrystallite voids (Pérez-Ramírez et al., 2008). Although the small-pore SOD zeolite is not proper to use as a support or catalyst, the nanosized SOD zeolite with the additional mesopore has the potential as support or catalyst in catalysis (Shanbhag et al., 2009; Hiyoshi, 2012).

The Si/Al ratio of the zeolite samples determined by ICP-OES and SEM-EDS are displayed in Table 4.1. The ratio from ICP-OES is from the whole sample, whereas that from SEM-EDS reflects the surface composition. The different values from both techniques might be from the presence of the amorphous phase which normally has a higher Si/Al ratio. The sample from the gel with a higher ethanol content tends to produce zeolite with a lower Si/Al ratio. Because the gel with more ethanol content has less water and NaOH is less soluble in ethanol, the gel with the more ethanol content has higher alkalinity. Thus, supersaturation of the synthesis gel is reached quickly leading to a faster nucleation and more Al incorporation. This result is supported by the literature that the higher alkalinity of the synthesis gel results in the more Al incorporation in the zeolite framework (Chatelaina et al., 1997; Ferchiche et al., 2001). The Si/Al ratio of the E00 sample is in the range of FAU zeolite. The Si/Al ratio of the sample E10 was nearly similar to that of EMT/FAU intergrowth in the literature (Chon et al., 1996). However, the Si/Al ratio of SOD (E50 and E60) in this work is higher than that in the literature (Gaber et al., 2019).

Table 4.1 Si/Al ratios, surface areas, and pore volumes of all samples.

Sample	Si/Al ratio		^a S _{BET} (m ² /g)	^b S _{Ext} (m ² /g)	^c V _{Mes} (cm ³ /g)	^d V _{Micro} (cm ³ /g)
	IPC-OES	SEM-EDX				
E00	1.87	1.45	637	113	0.10	0.26
E10	1.87	1.41	507	130	0.18	0.19
E20	1.71	1.30	431	193	0.62	0.12
E30	2.05	1.34	170	93	0.41	0.04
E40	1.71	1.33	132	66	0.38	0.03
E50	1.71	1.21	44	33	0.28	0.01
E60	1.43	1.26	30	30	0.14	0.00

^aS_{BET}: specific surface area determined by the BET method., ^bS_{Ext}: external surface area., ^cV_{Mes}: Mesopore volume determined by the BJH method., ^dV_{Mic}: Micropore volume calculated by the t-plot method

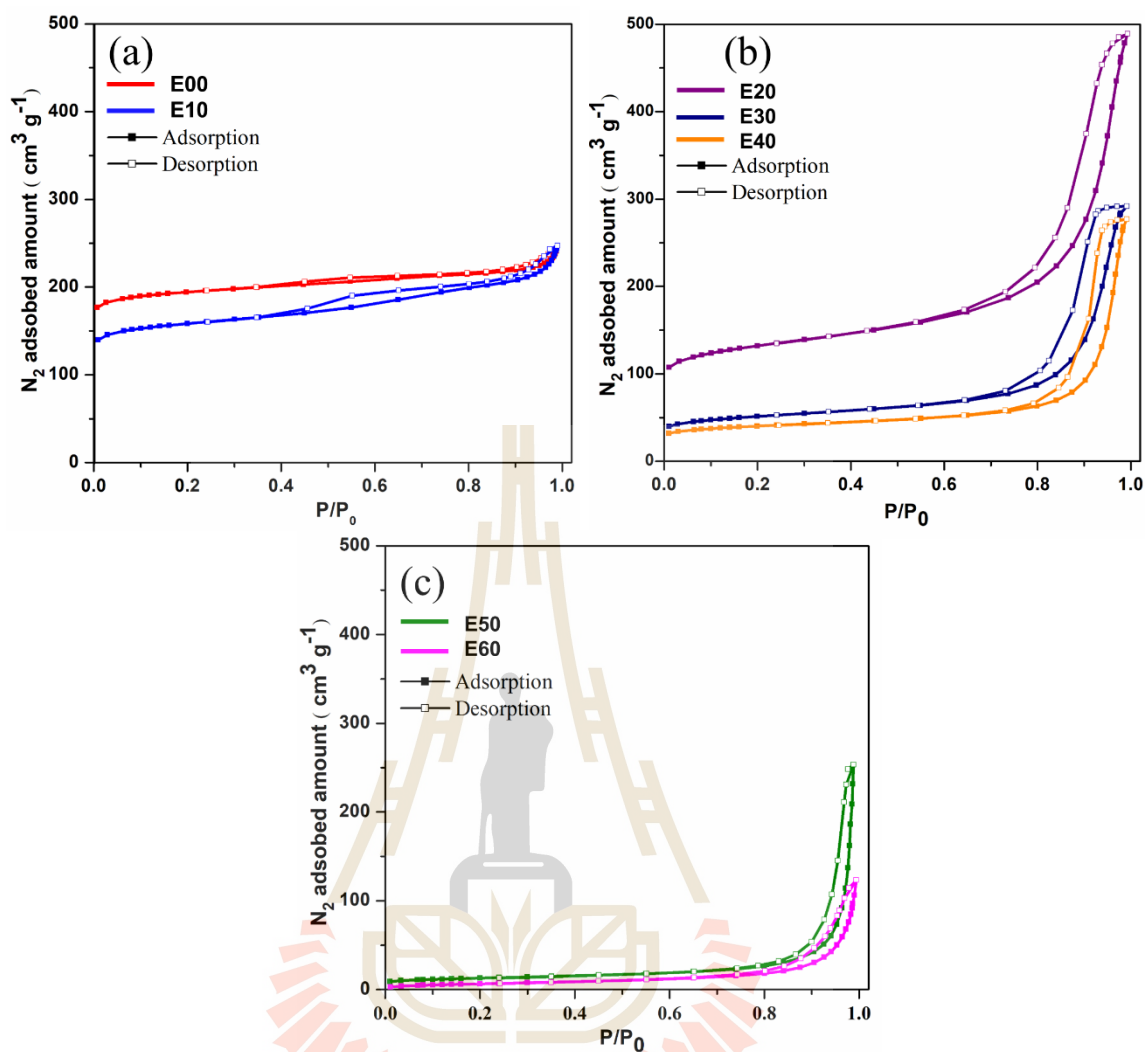


Figure 4.6 N_2 adsorption-desorption isotherms of (a) E00 and E10 samples, (b) E20, E30, and E40 samples, and (c) E50 and E60 samples.

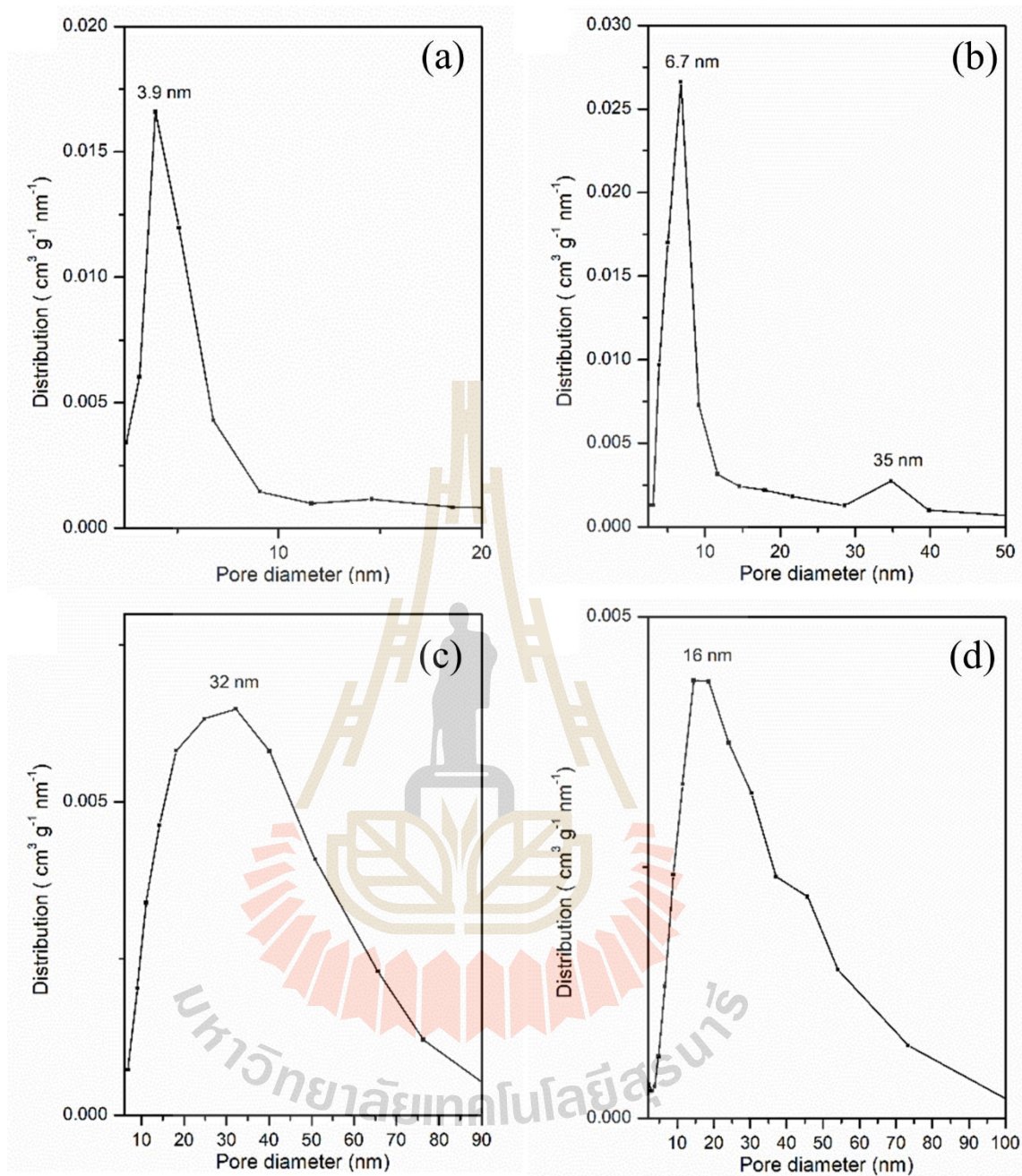


Figure 4.7 Pore size distribution of (a) E00, (b) E10, (c) E50, (d) E60 samples.

4.5 Thermal stability and water adsorption capacity of the samples

Thermogravimetric analysis (Figure 4.8(a)) and its first derivative (Figure 4.8(b)) curves of the E00, E10, E20 and E50 samples representing the FAU, EMT/FAU, mixed phases of the EMT/FAU and SOD, and SOD zeolites, respectively. The weight losses of the samples are in the range of 14.5-25.0%. The TGA and DTA curves of E00 and E10 have a similar feature which might be due to the similarity of their structures. Their weight losses are only at 150 °C due to loss of adsorbed waters in their surface, micro- and mesopores (Ahmad et al., 2016). The E00 and E10 zeolites are thermally stable up to 1000 °C indicating high thermal stability without their structure collision. However, the weight loss of the E00 (about 25%) is higher than that of the E10 (about 23%) which is consistent with the FTIR result.

The TG and DTG curves of the nanosized SOD zeolite from the E50 sample show three main peaks of weight losses. The two peaks about 120 and 250 °C are the loss of water molecules in β -cage while the peak at 820 °C are caused by phase transformation of SOD zeolite to nepheline and/or α -carnegieite (Khajavi et al., 2010; Fasolin et al., 2018). Normally, SOD zeolite has very low water adsorption capacity because water molecules cannot enter into its small pores. However, nanosized SOD zeolite in this work has a high water adsorption capacity of about 14.5% which could be from the presence of additional mesopores.

The DTA curve of the E20 sample exhibits the main peak at 150 °C and also observed a small shoulder peak at 120 and 250 °C. Moreover, the weight loss of this sample about 20.5% is between the weight losses of the EMT/FAU intergrowth and

SOD zeolites. These results indicate the mixing phases of EMT/FAU intergrowth and SOD zeolite in this sample.

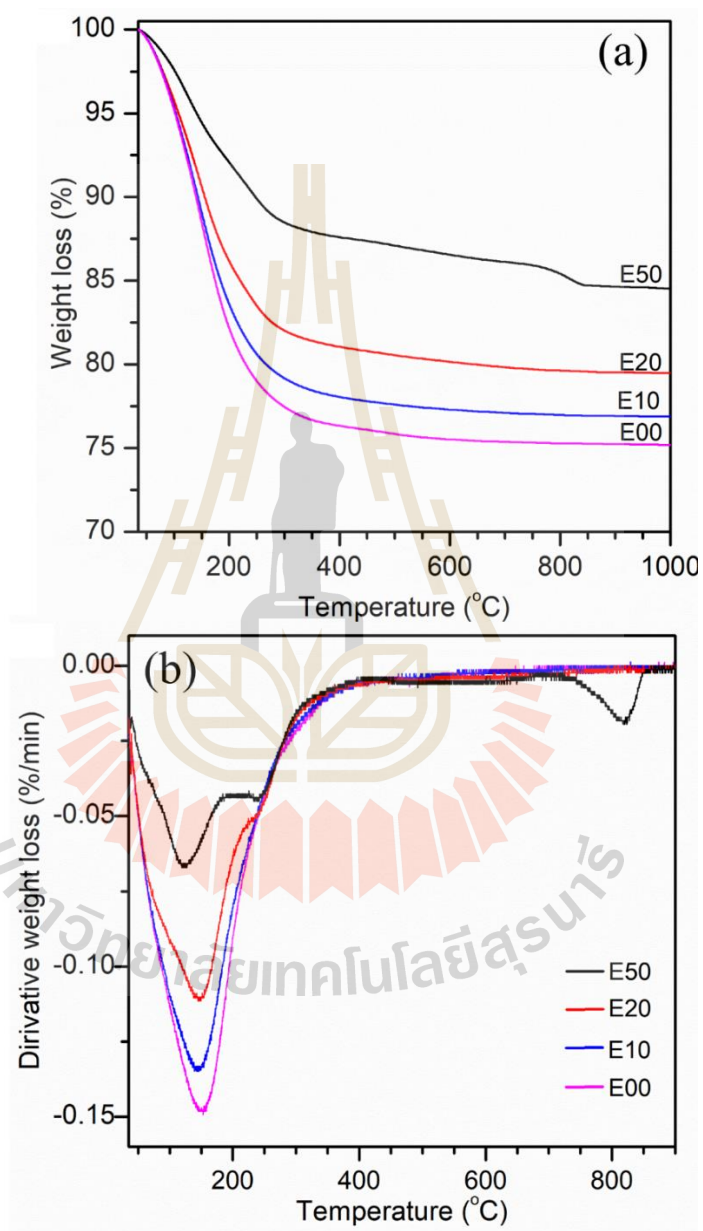


Figure 4.8 Thermogravimetric analysis of the synthesized samples including the E00 (magenta line), E10 (blue line), E20 (red line) and E50 (black line) samples. Panel (a) TGA and (b) DTA results.

4.6 References

- Ahmad, H. A., Bazin, P., Fernandez, C., Awala, H., and Mintova, S. (2016). Nanosized Na-EMT and Li-EMT zeolites : selective sorption of water and methanol studied by a combined IR and TG approach. **Physical Chemistry Chemical Physics**. 18: 30585–30594
- Belandría, L. N., González, C. S., Aguirre, F., Sosa, E., Uzcátegui, A., González, G., Brito, J., González-Cortés, S. L., and Imbert, F. E. (2008). Synthesis, characterization of FAU/EMT intergrowths and its catalytic performance in n-pentane hydroisomerization reaction. **Journal of Molecular Catalysis A: Chemical**. 281: 164–172.
- Chatelaina, T., Patarina, J., Brendl, E., Dogniera, F., Gutha, J. L., and Schulzb, P. (1996). Synthesis of high-silica FAU-, EMT-, RHO- and KFI-type zeolites in the presence of 18-crown-6 ether . **Progree in Zeolite and Microporous Materials**. 105: 173–180.
- Hums E. (2017). Synthesis of Phase-Pure Zeolite Sodalite from Clear Solution Extracted from Coal Fly Ash. **Journal of Thermodynamics & Catalysis**. 08: 1–6.
- Fasolin, S., Romano, M., Boldrini, S., Ferrario A., Fabrizio M., Armelao L., and Barison S. (2018). Single-step process to produce alumina supported hydroxy-sodalite zeolite membranes. **Journal of Materials Science**. 54:2049-2058.
- Ferliche, S., Warzywoda, J., and Jr, A. S. (2001). Direct synthesis of zeolite Y with large particle size. **International Journal of Inorganic Materials**. 3: 773–780.

- Gaber, S., Gaber, D., Ismail, I., Alhassan, S., and Khaleel, M. (2019). Additive-free synthesis of house-of-card faujasite zeolite by utilizing aluminosilicate gel memory. **CrystEngComm**. 21: 1685–1690.
- Gao, D., Duan, A., Zhang, X., Zhao, Z., E, H., Qin, Y., and Xu, C. (2015). Synthesis of CoMo catalysts supported on EMT/FAU intergrowth zeolites with different morphologies and their hydro-upgrading performances for FCC gasoline. **Chemical Engineering Journal**. 270: 176–186.
- Hiyoshi, N. (2012). Nanocrystalline sodalite: Preparation and application to epoxidation of 2-cyclohexen-1-one with hydrogen peroxide. **Applied Catalysis A: General**. 419–420: 164–169.
- Huang, Y., Yao, J., Zhang, X., Kong, C., Chen, H., Liu, D., Tsapatsis, M., Hill, M. R., Hill, A. J., and Wang, H. (2011). Role of ethanol in sodalite crystallization in an ethanol-Na₂O-Al₂O₃-SiO₂-H₂O system. **CrystEngComm**. 13: 4714–4722.
- Inayat, A., Schneider, C., and Schwieger, W. (2015). Organic-free synthesis of layer-like FAU-type zeolites. **Chemical communications**. 51: 279–281.
- Khajavi, S., Sartipi, S., Gascon, J., Jansen, J. C., and Kapteijn, F. (2010). Thermostability of hydroxy sodalite in view of membrane applications. **Microporous and Mesoporous Materials**. 132: 510–517.
- Khaleel, M., Wagner, A. J., Mkhoyan, K. A., and Tsapatsis, M. (2014). On the Rotational Intergrowth of Hierarchical FAU / EMT Zeolites. **Angewandte Chemie - International Edition**. 53: 9456–9461.

- Kimura, R., Wakabayashi, J., Elangovan, S. P., Ogura, M., and Okubo, T. (2008). Nepheline from K_2CO_3 /nanosized sodalite as a prospective candidate for diesel soot combustion. **Journal of the American Chemical Society**. 130: 12844–12845.
- Lohse, U., Pitsch, I., Schreier, E., Parlitz, B., and Schnabel, K. (1995). Cubic and hexagonal faujasites with varying Si / Al ratios I. Synthesis and characterization. **Applied Catalysis A: General**. 129: 189–202.
- Mintova, S., Jaber, M., and Valtchev, V. (2015). Nanosized microporous crystals : emerging applications. **Chemical Society Reviews**. 44: 7207–7233.
- Mintova, S., and Barrier, N. (2016). Verified syntheses of zeolitic materials. **Commission of the international zeolite association**.
- Möller, K., Yilmaz, B., Jacubinas, R. M., Müller, U., and Bein, T. (2011) One-step synthesis of hierarchical zeolite beta via network formation of uniform nanocrystals. **Journal of the American Chemical Society**. 133: 5284–5295.
- Ng, E. P., Chateigner, D., Bein, T., Valtchev, V., and Mintova, S. (2012). Capturing Ultrasmall EMT Zeolite from Template-Free Systems. **Science**. 335: 70–73.
- Nik, O. G., Chen, X. Y., and Kaliaguine, S. (2011). Amine-functionalized zeolite FAU / EMT-polyimide mixed matrix membranes for CO_2/CH_4 separation. **Journal of Membrane Science**. 379: 468–478.
- Pagis, C., Morgado Prates, A. R., Farrusseng, D., Bats, N., and Tuel, A. (2016). Hollow Zeolite Structures: An Overview of Synthesis Methods. **Chemistry of Materials**. 28: 5205–5223.

- Pérez-Ramírez, J., Christensen, C. H., Egeblad, K., Christensen, C. H., and Groen, J. C. (2008). Hierarchical zeolites: Enhanced utilisation of microporous crystals in catalysis by advances in materials design. **Chemical Society Reviews**. 37: 2530–2542.
- Petranovskii, V., Kiyozumi, Y., Kikuchi, N., Hayamisu, H., Sugi, Y., and Mizukami, F. (1996). The influence of mixed organic additives on the zeolites A and X crystal growth. **Progress in Zeolite and Microporous Materials**. 105: 149–156.
- Shanbhag, G. V., Choi, M., Kim, J., and Ryoo, R. (2009). Mesoporous sodalite: A novel, stable solid catalyst for base-catalyzed organic transformations. **Journal of Catalysis**. 264: 88–92.
- Treacy, M. M. J., Vaughan, D. E. W., Strohmaier, K. G., and Newsam, J. M. (1996). Intergrowth segregation in FAU-EMT zeolite materials. **Proceedings of the Royal Society of London A**. 452: 813–840.
- Yao, J., Zhang, L., and Wang, H. (2008). Synthesis of nanocrystalline sodalite with organic additives. **Materials Letters**. 62: 4028–4030.
- Zhou, Y., Chen, W., Wang, P., and Zhang, Y. (2018). EMT-type zeolite for deep purification of trace polar-oxygenated compounds from light olefins. **Microporous and Mesoporous Materials**. 271: 273–283.

CHAPTER V

CONCLUSIONS

It is demonstrated in this thesis that the FAU, EMT/FAU intergrowth and SOD zeolite with different shapes and sizes can be obtained from the synthesis gel of zeolite NaX by tuning the ethanol/water ratio. The ethanol/water molar ratio plays an important role in the zeolite phase, morphology, and crystallization process. XRD and FTIR reveal that the ethanol/water molar ratio of 0.045 promotes crystallization of large pore EMT/FAU intergrowth. The ethanol/water ratios of 0.412 and 0.628 favor the crystallization of SOD zeolite. SEM and TEM show that the morphologies of EMT/FAU intergrowth are hollow and undefined shapes while that of SOD zeolite is polycrystals. SEM-EDX and ICP-OES confirm that the increase of ethanol/water ratio results in the lower Si/Al ratio of the obtained zeolites because it leads to high alkalinity which facilitates Al incorporation in the zeolite structure. N₂ sorption analysis shows that the additional mesopores in the samples resulting from the agglomeration of small or nanosized zeolite crystals. The template-free method with a short time and low temperature in this study might provide an alternative route to synthesize the intergrowth of EMT/FAU and SOD zeolites. Additionally, a better understanding of the effect of ethanol on the zeolite phase, morphology and porosity might offer an optional way to control phase and morphology of other zeolites in the future.

CURRICULUM VITAE

Nawee Jantarit

Address 118 No.6, Klang Sub-district, Detudom District, Ubon
Ratchathani, Thailand, 34160 Email: nawee1995@gmail.com

Education

2017 B.Sc. (Chemistry) with first class honors
Suranaree University of Technology (SUT), Nakhon
Ratchasima, Thailand

2017- 2019 Student in M.Sc. program in Chemistry, SUT

Scholarship

2013-Present Development and Promotion of Science and Technology
Talents Project (DPST)

มหาวิทยาลัยเทคโนโลยีสุรนารี